Conception of a topological analogue of the magnetic bit

by

Xinyuan Xu

Master's thesis submitted to

Faculté des Sciences, Université de Sherbrooke
Sherbrooke, Québec, Canada

Le *** 2022

le jury a accepté le mémoire de Monsieur Xinyuan Xu dans sa version finale.

Membres du jury

P^{r} Ion Garate
Co-directeur de recherche
Département de physique

P^{r} David Sénéchal
Co-directeur de recherche
Département de physique

P^{r} Alexandre Blais
membre interne
Département de physique

P^{r} René Côté
Président rapporteur
Département de physique

Contents

List of Figures

Chapter 1

Introduction

1.1 Topological phases

Over the last 15 years, there has been an explosion of research activity in topological condensed matter physics [5, 10, 11, 20, 21], numerous papers related to topological phases have been published.

Topological phases are exotic phases of matter characterized by a set of integer numbers known as topological invariants. These integers capture the topology of the electronic wave functions in momentum space (e.g. the winding number of the phase of the wave function along the Brillouin zone edge) [31]. Generally, nonzero topological invariants manifest themselves physically through the appearance of robust gapless (metallic) electronic states at the boundaries of the material. Two celebrated examples of this phenomenon are the quantum Hall insulator [3] and the quantum spin Hall insulator [10]; see Figs. (1.2)and (1.1).

In recent years, a keen interest has emerged to control and alter the values of topological invariants through the application of external perturbations [23]. A general mechanism to change a topological invariant is the "band inversion" [27]. A graph illustration of the band inversion mechanism is given in Fig. (1.3). In the language of band theory, in order to change the topology while preserving the symmetries of the system, one needs to close the energy gap and then reopen it with the opposite band ordering. In the inverted regime, a small fraction of the valence band goes to the conduction band, and a small fraction of the conduction band goes to the valence band. As a consequence, the boundary of the system has a metallic state and the bulk is insulating. It must be noted that, in certain systems, one can realize a band inversion without having to go through a closure of the energy gap. This situation takes place when the topological invariant is protected by a symmetry and the external perturbation breaks that symmetry. In chapter 4 of this thesis, we will be dealing with precisely such a situation.

The band inversion mechanism is quite general, but it does not tell us the dynamics of order parameter during this process, which will be the main focus of this thesis.

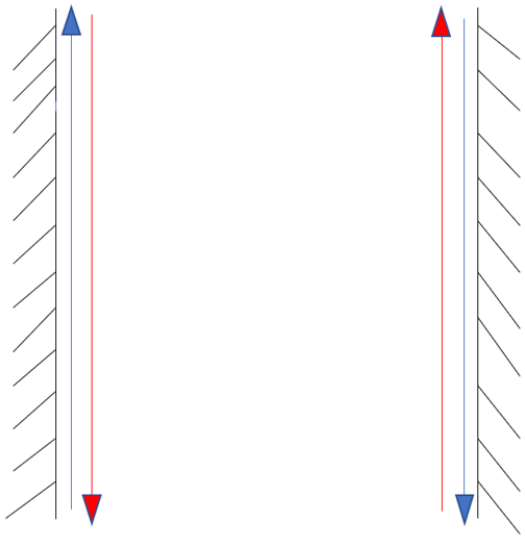

Figure 1.1
Edge states of the 2D quantum spin hall insulator. The current in blue is carried by electrons with spin $1/2$ and the current in orange is carried by electrons with spin $-1/2$. The gapless edge state is protected by time-reversal symmetry and is characterized by a $\mathscr{Z}_2$ topological invariant.

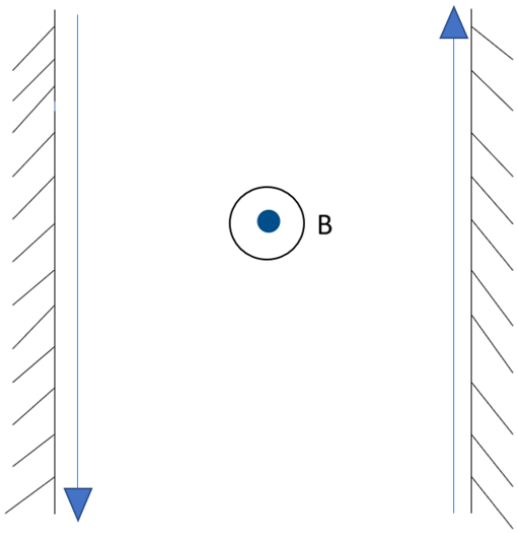

Figure 1.2
Edge state in a quantum hall insulator. The current in blue is carried by electrons. There is a magnetic field perpendicular to the plate. The gapless edge state is a consequence of time-reversal symmetry breaking.

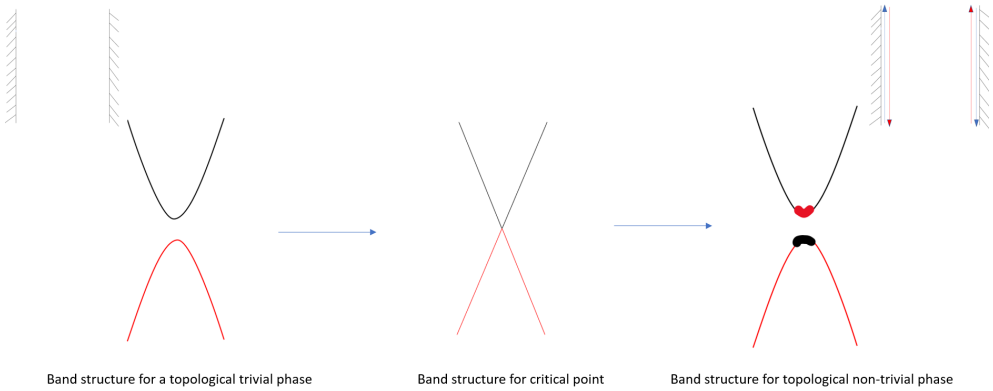

Figure 1.3
Schematic description of a band inversion. On the left panel, the system is a normal or topologically trivial insulator, in the sense that its band structure can be adiabatically deformed (i.e. without the closure of the energy gap) toward the band structure of vacuum. In this case, there is no gapless edge modes (top left inset). By closing the energy gap (middle panel) and reopening it again with inverted band ordering (right panel), the band structure is no longer adiabatically connected to that of vacuum and consequently there is a gapless state at the sample boundary (top right inset).

1.2 Floquet engineering

A widely accepted way to achieve a band inversion with the application of external perturbations is through Floquet engineering. In this scheme,the band structure is modified by a periodic driving and a band inversion is included in the Floquet Hamiltonian. In some systems, this could be achieved by coupling the system to polarized light [30]. A graph presentation of Floquet engineering is given in Fig. (1.4).

In Floquet engineering, the Hamiltonian of the system is periodic in time T: $H(t) = H(t+T)$. Generally, the topological invariant is computed by using the Bloch states $|u_{kn}(\mathbf{r})\rangle$ [10], which form a static, complete orthogonal set of solutions for the time-independent Schrodinger equation. For instance, in one dimension, the topological invariant for the electronic band n is given by [10]

$$N = \frac{1}{2\pi}\oint dk\langle u_{kn}|i\partial_k|u_{kn}\rangle, \tag{1.1}$$

where the integral in the wave vector k is along the entire Brillouin zone. However, in Floquet engineering we use a time-dependent basis $|\Phi(t)\rangle$, where $\exp(-i\tilde{\epsilon}t)|\Phi(t)\rangle$ forms a complete orthogonal set of solutions for the time-dependent Schrodinger equation, $\tilde{\epsilon}$ is the generalized energy and $|\Phi(t)\rangle = |\Phi(t+T)\rangle$. The one-period time evolution operator can be defined as

$$U(T,k) = \exp\left(-i\int_0^T dt' H(t',k)\right) \equiv exp(-iH_{\text{eff}}(k)T), \tag{1.2}$$

where $H_{\text{eff}}(k)$ is an effective time-independent Hamiltonian known as the Floquet Hamiltonian. The topological invariant for the periodically driven system can be calculated directly from $H_{\text{eff}}(k)$, similarly as it is done in equilibrium (e.g. using Eq. (1.1) if the system is one dimensional in space).

Let us suppose that the initial (equilibrium) Hamiltonian is topologically trivial. Accordingly, the band structure of the initial Hamiltonian does not display inverted bands. Now, for an appropriate external drive, H_{eff} can host inverted bands. When that happens, we say that the topological invariant has been changed due to the external periodic perturbation.

One conceptual and practical limitation of Floquet engineering is that its effect is transient. In other words, once the external drive is switched off, the system goes back to its initial state (e.g. to the topologically trivial state in the example considered in the preceding paragraph). This limitation motivates the main question of the present thesis: is it possible to conceive a system in which a small transient external perturbation can lead to a permanent change in the electronic band topology? If the answer to this question is affirmative, we will have conceived a topological analogue of the magnetic bit.

1.3 Magnetic bit and the Landau-Lifshitz-Gilbert equation

The magnetization of an easy-axis ferromagnet forms a “magnetic bit”, which is the basis for magnetic memories in today’s information technology [35]. A magnetic bit consists of two energetically degenerate magnetization confirgurations, labeled as "0" state and "1" state. These two magnetic states minimize the energy of the ferromagnet. In order to go from one energy minimum to another by changing the direction of the magnetization, there is an energy cost known as the magnetic anisotropy energy. This energy barrier ensures the stability of the magnetic memory. A graph presentation of the magnetic bit is given in Fig. (1.5).

It is well-known that a transient small external perturbation can lead to a permanent change from the "0" state to the "1" state permanently, This is necessary in order to write new data in the magnetic memory. A graph presentation of the process is given in Fig. (1.6). The dynamics of such process is described by the Landau-Lifshitz-Gilbert equation [2]:

$$\frac{d\mathbf{M}}{dt} = -\gamma \mathbf{M} \times \mathbf{H}_{\text{eff}} - \lambda \mathbf{M} \times (\mathbf{M} \times \mathbf{H}_{\text{eff}}), \tag{1.3}$$

and

$$\mathbf{H}_{\text{eff}} = \mathbf{H}_{\text{ext}} + \mathbf{H}_{\text{ani}}, \tag{1.4}$$

where $\mathbf{M}$ is the magnetism of the system in the mean-field approximation, $\mathbf{H}_{\text{eff}}$ is the effective magnetic field (perturbation), $\mathbf{H}_{\text{ext}}$ is the external magnetic field and $\mathbf{H}_{\text{ani}}$ is the magnetic anisotropy field (obtained by taking the derivative of the anisotropy energy with respect to the magnetization direction). The first term in the right-hand side

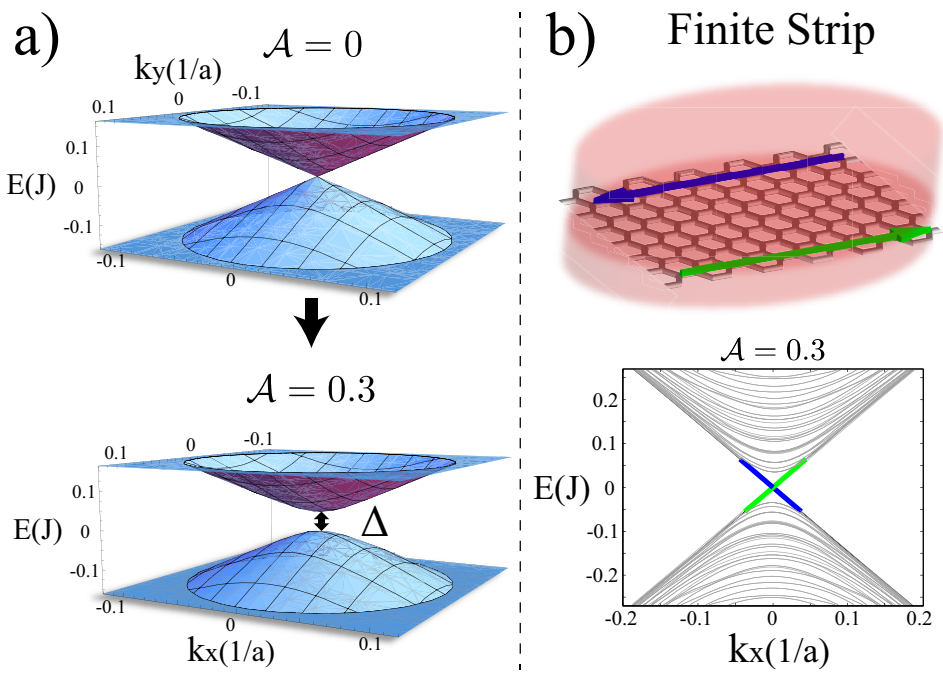

Figure 1.4
Example of Floquet engineering of topological phases. The equilibrium bulk band structure is displayed in the top of panel (a). It describes a strip of graphene with armchair edges, which is topologically trivial. The bottom of panel (a) shows the bulk band structure under light irradiation. The system now has bands with nonzero topological invariants, which manifest themselves through the appearance of metallic edge states (panels (b) and (c)). Figure taken from [23].

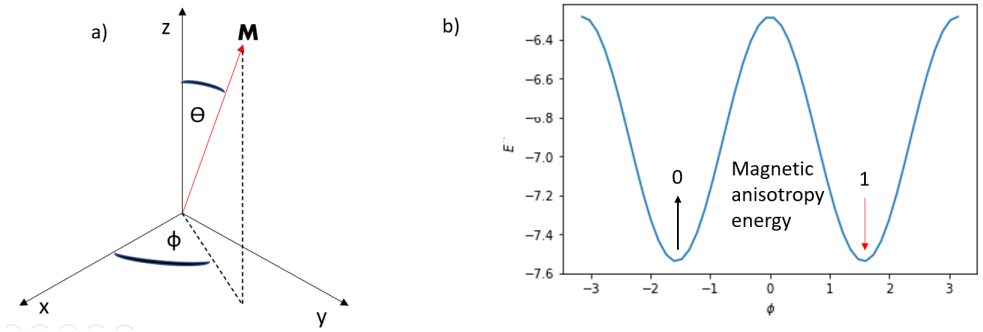

Figure 1.5
Schematic representation of a magnetic bit. (a) Magnetization of a ferromagnet, with polar and azimuthal angles θ and ϕ. (b) Cartoon of the energy of an easy-axis ferromagnet as a function of ϕ. There are two degenerate local minima, which describe the two states of the magnetic bit ("0" and "1"). The energy barrier between the two states is the magnetic anisotropy energy.

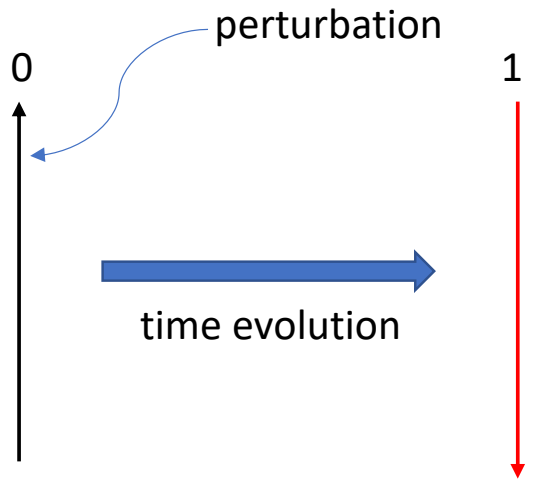

Figure 1.6
Cartoon of magnetization switching produced by an external perturbation.

describes the precession of the magnetism around the effective magnetic field with a gyromagnetic ratio γ, the second term in the right-hand side describes the damping relaxation of the magnetization towards the effective magnetic field via damping of amplitude λ. Damping is essential in order for the magnetization to settle into the new energy minimum once the external perturbation is switched off. Likewise, magnetic anisotropy energy is essential to ensure that the final state will be stable and that the system will not return to its initial state once the perturbation is swicthed off.

In this thesis, we intend to describe a counterpart of the magnetic bit and the Landau-Lifshitz-Gilbert equation for a topological phase, where the role of 0 and 1 is played by two states of different topological invariants. This is an example of dynamics and control of topological invariants that goes beyond the Floquet engineering.

In order to provide a proof-of-principle for the topological analogue of a magnetic bit, we will work on the simplest possible model that gathers all the necessary ingredients, namely: (i) energetically degenerate ground states with differing values of the topological invariants, (ii) an analogue of the magnetic anisotropy energy, (iii) an analogue of external magnetic fields. This model, known as the SSH-Holstein model, will be introduced in the next chapter.

A graph presentation of the Landau-Lifshitz-Gilbert equation is given in Fig. (1.7). We notice that Eq. (1.3) is only approximate, appropriate for slow-enough dynamics of the magnetization. In addition, Eq. (1.3) conserves the magnitude of the magnetization; only its direction is susceptible to change. This is a good approximation for many ferromagnets at temperatures well below the Curie temperature, where the energetic cost of changing the direction of magnetization (a consequence of spin-orbit interactions) is far less than the energy required to change the magnitude of the magnetization.

We map the order parameter to the magnetism, and we will derive a topological

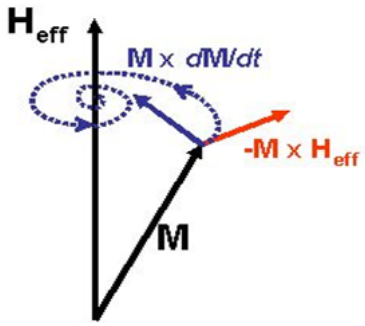

Figure 1.7
A pictorial presentation of the Landau-Lifshitz-Gilbert equation.The red trajectory describes the precession, and the blue trajectory describes the damping relaxation. The figure is taken from Wikipedia (See the Wikipedia article on the "Landau–Lifshitz–Gilbert equation").

analogue equation of the Landau-Lifshitz-Gilbert equation. This is an example of beyond Floquet engineering.

Chapter 2

SSH-Holstein model

In this chapter, we present and explain the SSH-Holstein model. We begin by reviewing the SSH and Holstein models separately, and by describing the band topology in each case. The SSH-Holstein model is then constructed. This model will be used in later chapters for a proof-of-principle realization of the topological bit.

2.1 The SSH model

In its simplest realization, the SSH model describes spinless electrons moving in one dimension with a hopping amplitude modulated by phonons. Its Hamiltonian is given by [33]

$$H_{\mathrm{SSH}} = t_0 \sum_j (c_j^\dagger c_{j+1} + h.c.) - \alpha_S \sum_j (q_j - q_{j+1})(c_j^\dagger c_{j+1} + H.c.) + \frac{1}{2} m_S \sum_j \Big[(\dot{q}_j - \dot{q}_{j+1})^2 + \omega_S^2 (q_j - q_{j+1})^2 \Big], \tag{2.1}$$

where t_0 is the hopping between nearest sites, q_j is the lattice displacement at site j and α_S is the SSH electron-phonon coupling constant. We assume t_0 is real. At half-filling (one electron per two sites), the system undergoes a Peierls instability towards a gapped bond density wave [22]. In the mean-field approximation, the density wave is described by $q_j = (-1)^j \Delta_{0x}/2$, where Δ_{0x} is a static order parameter. When substituting this order parameter in Eq. (2.1), the hopping amplitude becomes dimerized, so

$$H_{\mathrm{SSH,MF}} = t_0 \sum_j (c_j^\dagger c_{j+1} + H.c.) - \alpha_S \Delta_{0x} \sum_j (-1)^j (c_j^\dagger c_{j+1} + h.c.) + \frac{1}{2} m_S \omega_S^2 \sum_j \Delta_{0x}^2. \tag{2.2}$$

A geometric presentation of the SSH model is given in Fig. (2.1). In pseudospin representation, the bond density wave can be mapped onto an antiferromagnetic state.

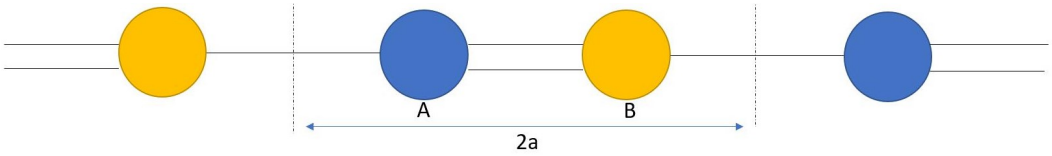

Figure 2.1
Schematic representation of the mean-field ground state of the SSH model. The hopping amplitude is modulated between weak and strong values (single and double lines, respectively). As a result the system has a two-atom unit cell. The two sites in the unit cell are denoted as A and B sites (in blue and yellow, respectively).

To see this we define the pseudospin operators

$$\begin{aligned} S_j^z &= c_j^\dagger c_j - c_{j+1}^\dagger c_{j+1} \\ S_j^x &= c_j^\dagger c_{j+1} + c_{j+1}^\dagger c_j \\ S_j^y &= -ic_j^\dagger c_{j+1} + ic_{j+1}^\dagger c_j. \end{aligned} \tag{2.3}$$

Then, $\langle S_{j+1}^x \rangle \propto (-1)^{j+1}\alpha_S \Delta_{0x}$, and Δ_{0x} can be understood as a Néel order along x. The mapping between the bond density wave order parameter and the magnetic order parameter motivates our later approach of borrowing from the concepts of spintronics in order to determine the dynamics of the density-wave order parameter.

Adopting periodic boundary conditions, Eq. (2.2) can be written in Fourier space as

$$H_{\text{SSH,MF}} = \sum_{k_1} \begin{bmatrix} C_{k_1 A}^\dagger & C_{k_1 B}^\dagger \end{bmatrix} \mathbf{d}_{k_1} \cdot \boldsymbol{\sigma} \begin{bmatrix} C_{k_1 A} \\ C_{k_1 B} \end{bmatrix} + \frac{N}{2} K_S \Delta_{0x}^2, \tag{2.4}$$

we will use k_1 for wavenumber and k_0 for frequency. A and B denote the two sites in a unit cell, N is the number of sites, $K_S = m_S \omega_S^2$ is the phonon stiffness. $C_{k_1,A}^\dagger$ and $C_{k_1,B}^\dagger$ are the electronic creation operator of A and B sites respectively; $C_{k_1,A}$ and $C_{k_1,B}$ are the electronic annihilation operator of A and B sites respectively. Vector d is

$$\begin{aligned} d_x &= (t_0 + \alpha_S \Delta_{0x}) + (t_0 - \alpha_S \Delta_{0x}) \cos(2k_1 a) \\ d_y &= -(t_0 - \alpha_S \Delta_{0x}) \sin(2k_1 a) \\ d_z &= 0, \end{aligned} \tag{2.5}$$

and a is the lattice constant. The dispersion relation of the electrons is then

$$\epsilon_{k_1 \pm} = \pm \sqrt{2(t_0^2 + \alpha_S^2 \Delta_{0x}^2) + 2(t_0^2 - \alpha_S^2 \Delta_{0x}^2) \cos(2k_1 a)}, \tag{2.6}$$

and its spectrum is shown in Fig. (2.2). We expand the energy around the vicinity of

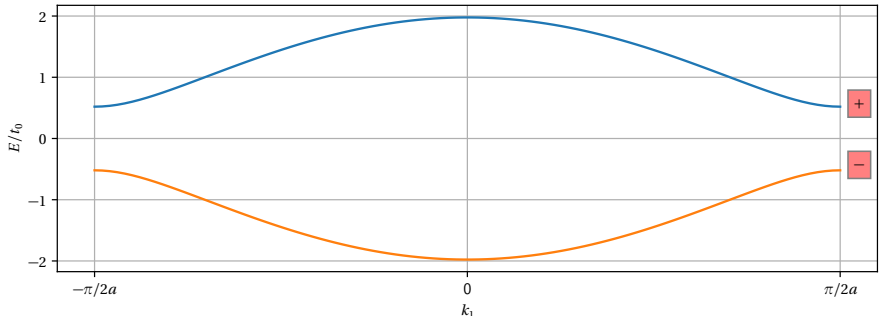

Figure 2.2
Energy spectrum of the SSH model, where "+" labels the conduction band, and "−" labels the valence band. We choose $a = 1$ and $\alpha_S \Delta_{0x}/t_0 = 0.3$.

the two Fermi points $k_1 = \frac{\pi}{2a} + q_1$, so the ground state energy of the system is

$$\begin{aligned} E[\Delta_{0x}] &\approx -\sum_{q_1} \sqrt{4a^2 t_0^2 q_1^2 + 4\alpha_S^2 \Delta_{0x}^2} + \frac{N}{2} K_S \Delta_{0x}^2 \\ &= -\frac{Na}{2\pi} \int dq_1 \sqrt{4a^2 t_0^2 q_1^2 + 4\alpha_S^2 \Delta_{0x}^2} + \frac{N}{2} K_S \Delta_{0x}^2 \end{aligned} \tag{2.7}$$

the mean-field energy and order parameters are obtained by minimizing the energy, i.e, imposing $\partial E/\partial \Delta_{0x} = 0$. By doing this we get

$$\Delta_{0x} = \pm \frac{2a t_0 \Lambda}{\alpha_S} \exp - \frac{\pi t_0 K_S}{2\alpha_S^2}, \tag{2.8}$$

where Λ is a momentum cutoff. Even though this value of Δ_{0x} minimizes the energy, $\Delta_{0x} = 0$ is also a solution but corresponds to a higher energy state in one dimension. At the mean field level there are only two possible values of Δ_{0x} and they only differ by a sign. This is an example of commensurate charge density wave (coomensurate CDW).

The eigenvectors of the conduction band "+" and valence band "−" are

$$|+, k_1\rangle = \begin{bmatrix} \cos\frac{\theta}{2} \\ e^{i\varphi} \sin\frac{\theta}{2} \end{bmatrix} \qquad |-, k_1\rangle = \begin{bmatrix} -\sin\frac{\theta}{2} \\ e^{i\varphi} \cos\frac{\theta}{2} \end{bmatrix}, \tag{2.9}$$

where $\theta = \arccos(d_z/\sqrt{d_x^2 + d_y^2 + d_z^2})$ and $\varphi = \arctan(d_y/d_x)$. In SSH model $\theta = \pi/2$ because $d_z = 0$.

It is clear that the energy spectrum is invariant under a sign change of Δ_{0x}. However the sign of Δ_{0x} has impact on the band topology of the system. To see this, let us calculate the Berry phase for the SSH Hamiltonian in the mean-field approximation. The Berry phase is a geometric phase that appears in quantum mechanical system. It only depends on the closed path of the external parameter [6] in parameter space. When

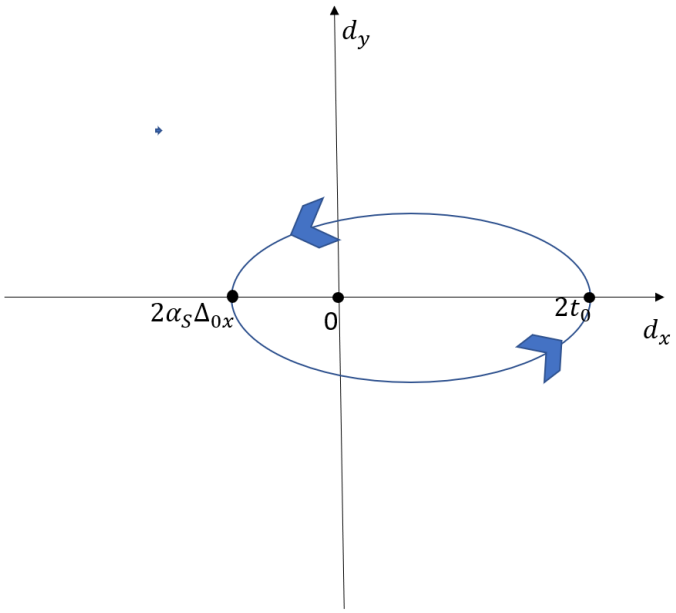

Figure 2.3
Schematic representation of the winding number of the SSH model, for the case of $\Delta_{0x} < 0$. The blue line describes the closed path made by when k_1 varies from $-\pi/2a$ to $\pi/2a$. The angle φ defined by $\tan\varphi = d_y/d_x$ completes a full circle and therefore the winding number is one.

the parameter is the crystal momentum this phase is called the "Zak phase" [10]. The Zak phase is related to the electronic transport property of an insulator [36]. For the SSH model the Berry phase is [10]

$$\begin{aligned}\gamma_\pm &= i\int_{-\frac{\pi}{2a}}^{\frac{\pi}{2a}} dk_1 \langle \pm, k_1 | \partial_{k_1} | \pm, k_1 \rangle = -\frac{1}{2}\int_{-\frac{\pi}{2a}}^{\frac{\pi}{2a}} dk_1 \partial_{k_1}\varphi \\ &= -\frac{1}{2}\Big[\varphi\left(\frac{\pi}{2a}\right) - \varphi\left(\frac{-\pi}{2a}\right)\Big] = -n\pi.\end{aligned}$$

Since $\pi/2a$ and $-\pi/2a$ are the same point, the single value property of the wave function implies that $\varphi\left(\frac{\pi}{2a}\right) - \varphi\left(\frac{-\pi}{2a}\right)$ must be a multiple of 2π. The multiplicity n is the winding number (the number of loops made by φ as k_1 covers the Brillouin zone.) For $\Delta_{0x} < 0$, it turns out that $n = 1$ and therefore the Berry phase is $\pi \,(\mathrm{mod}\, 2\pi)$; for $\Delta_{0x} > 0$, $n = 0$ and the Berry phase is $0\,(\mathrm{mod}\, 2\pi)$. This is because the minimum value of d_x is equal to $2\alpha_S\Delta_{0x}$. See Fig. (2.3) and Fig. (2.4).

In the SSH model chiral symmetry is preserved because $[H, \sigma^z]_+ = 0$ ($[\cdot,\cdot]_+$ is the anti-commutator). There is a robust electron edge state, the Jackiw-Rebbi zero mode [10]. As long as chiral symmetry is preserved, the edge mode will always be present [10] in finite-size chains, provided that the winding number therein is nonzero.

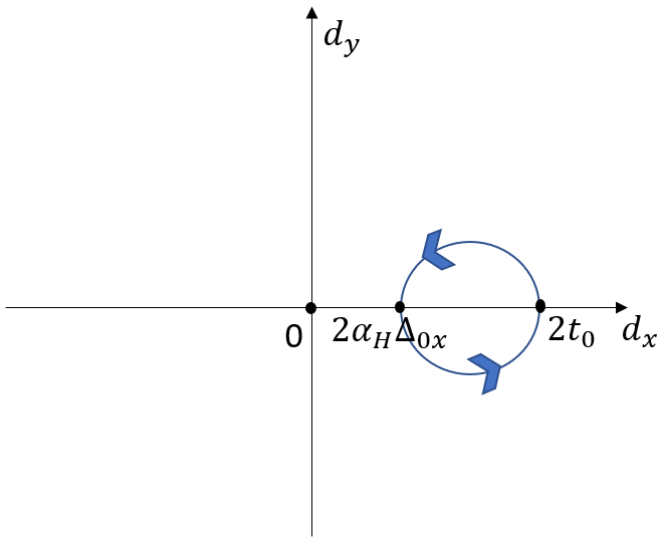

Figure 2.4
Schematic representation of the winding number of the SSH model, for the case of $\Delta_{0x} > 0$. The blue line describes the closed path made by when k_1 varies from $-\pi/2a$ to $\pi/2a$. The angle φ defined by $\tan\varphi = d_y/d_x$ does not complete a circle and therefore the winding number is zero.

This is an example of symmetry-protected topological phase [31]. The physical interpretation of the existence of the edge state is that a non-trivial Zak phase is related to the non-trivial bulk polarization, so the edge state must carry charge.

2.2 The Holstein model

In its simplest realization, the Holstein model describes spinless electrons moving in one dimension with an onsite potential modulated by phonons. Its Hamiltonian is given by [17]

$$H_{\text{Holstein}} = t_0 \sum_j (c_j^\dagger c_{j+1} + H.c.) - \alpha_H \sum_j Q_j (c_j^\dagger c_j) + \frac{1}{2} m_H \sum_j \left[\dot{Q_j}^2 + \omega_H^2 Q_j^2 \right], \quad (2.10)$$

where Q_j is the lattice displacement at site j and α_H is the Holstein electron-phonon coupling constant. We work in a gauge where t_0 is real. At half filling, the system undergoes a Peierls instability towards a gapped site-density wave [17]. In mean field approximation, the density wave is defined by $Q_j = \frac{(-1)^j}{2}\Delta_{0z}$, where Δ_{0z} is a static order

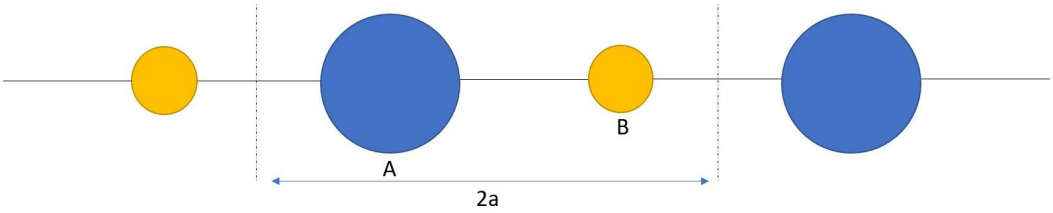

Figure 2.5
Schematic representation of the mean-field ground state of the Holstein model. The site potential is modulated between weak and strong values (single and double lines, respectively). As a result the system has a two-atom unit cell. The two sites in the unit cell are denoted as A and B sites (in blue and yellow, respectively).

parameter. It follows that the onsite potential becomes dimerized, so

$$H_{\text{Holstein,MF}} = t_0 \sum_j (c_j^\dagger c_{j+1} + h.c.) - \frac{1}{2}\alpha_H \Delta_{0z} \sum_j (-1)^j (c_j^\dagger c_j - c_{j+1}^+ c_{j+1}) + \frac{1}{2} m_H \omega_H^2 \sum_j \Delta_{0z}^2. \tag{2.11}$$

A geometric presentation of the Holstein model is given in Fig. (2.5). In the pseudospin representation, the site density wave can also be mapped onto an antiferromagnetic state by the same operators as in Eq. (2.3). Then, $\langle S_{j+1}^z \rangle \propto (-1)^{j+1} \alpha_H \Delta_{0z}/2$, and Δ_{0z} can be understood as a Néel order along z.

In Fourier space the Hamiltonian can be written as

$$H_{\text{Holstein,MF}} \approx \sum_{k_1} \begin{bmatrix} C_{k_1 A}^\dagger & C_{k_1 B}^\dagger \end{bmatrix} \mathbf{d} \cdot \boldsymbol{\sigma} \begin{bmatrix} C_{k_1 A} \\ C_{k_1 B} \end{bmatrix} + \frac{N}{2} K_H \Delta_{0z}^2, \tag{2.12}$$

where

$$\begin{aligned} d_x &= t_0 + t_0 \cos(2k_1 a) \\ d_y &= -t_0 \sin(2k_1 a) \\ d_z &= \alpha_H \Delta_{0z}. \end{aligned} \tag{2.13}$$

A, B denotes sites within one unit cell and $K_H = m_H \omega_H^2$ is the phonon stiffness.The dispersion relation of the electrons is

$$\epsilon_{k_1} = \pm \sqrt{\alpha_H^2 \Delta_{0z}^2 + 2t_0^2 + 2t_0^2 \cos(2k_1 a)}, \tag{2.14}$$

and its energy spectrum is shown in Fig. (2.6). The ground state energy of the system at half-filling is

$$E[\Delta_{0z}] \approx -\sum_{q_1} \sqrt{4a^2 t_0^2 q_1^2 + \alpha_H^2 \Delta_{0z}^2} + \frac{N}{2} K_H \Delta_{0z}^2, \tag{2.15}$$

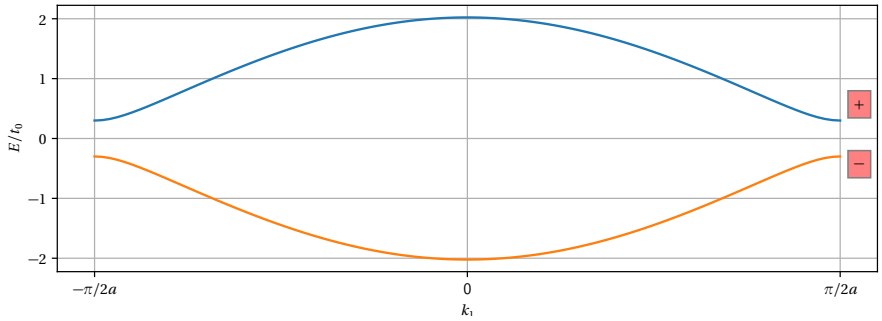

Figure 2.6
Energy spectrum of the Holstein model, where "+" means the conduction band, "-" means the valence band. We choose $a = 1$ and $\alpha_H^2 \Delta_{0z}^2 = 0.09$.

Again the mean-field order parameter can be obtained by minimizing the energy:

$$\Delta_{0z} = \pm \frac{4at_0\Lambda}{\alpha_H} \exp -\frac{2\pi t_0 K_S}{\alpha_H^2}, \tag{2.16}$$

where Λ is a UV (ultraviolet) momentum cutoff. $\Delta_{0z} = 0$ is also a solution by minimizing the energy, however $\Delta_{0z} = 0$ always corresponds to a higher energy state in one dimension. At the mean-field level there are only two possible value of Δ_{0z} and they only differ by a sign.

The Berry phase can still be obtained from E.q (2.9), this time with $\mathbf{d}$ given by Eq. (2.13):

$$\gamma_\pm = i \int_{-\frac{\pi}{2a}}^{\frac{\pi}{2a}} dk_1 \langle \pm, k_1 | \partial_{k_1} | \pm, k_1 \rangle = -\frac{1}{2}\Big[\varphi\left(\frac{\pi}{2a}\right) - \varphi\left(\frac{-\pi}{2a}\right)\Big] - \frac{1}{2}\int_{-\frac{\pi}{2a}}^{\frac{\pi}{2a}} dk_1 \partial_{k_1} \varphi \cos\theta,$$

the Berry phase could be an arbitary value depending on the value of $\alpha_H \Delta_{0z}$. Δ_{0z} and $-\Delta_{0z}$ have the same energy, besides Δ_{0z} and $-\Delta_{0z}$ both have no well-defined Berry phase so there is no robust electron edge state since the chiral symmetry is broken.

Both the SSH state and the Holstein state of the CDW (charge density wave) break a discrete symmetry. With periodic conditions, this symmetry is $q_j \to q_{j+1}$ and $c_j \to c_{j+1}$ (translation by one lattice site). The formation of the SSH or the Holstein ground state costs elastic energy, but the gain in kinetic energy is larger, so they form stable ground state.

2.3 SSH-Holstein model

Combining Eqs. (2.1) and Eqs. (2.10), we obtain the Hamiltonian of the SSH-Holstein model:

$$H = t_0 \sum_j (c_j^\dagger c_{j+1} + h.c.) - \alpha_S \sum_j (q_j - q_{j+1})(c_j^\dagger c_{j+1} + h.c.) - \alpha_H \sum_j Q_j (c_j^\dagger c_j) + \frac{1}{2} m_S \sum_j \left[(\dot{q}_j - \dot{q}_{j+1})^2 + \omega_S^2 (q_j - q_{j+1})^2 \right] + \frac{1}{2} m_H \sum_j \left[\dot{Q}_j{}^2 + \omega_H^2 Q_j^2 \right]. \tag{2.17}$$

Based on the preceding sections, we propose the mean fields

$$q_j = \frac{(-1)^j}{2} \Delta_{0x}$$
$$Q_j = \frac{(-1)^j}{2} \Delta_{0z}. \tag{2.18}$$

Like before, the values of the mean fields can be obtained by minimizing the energy. At half filling, we can show that the energy of the system is

$$E[\Delta_{0x}, \Delta_{0z}] = -\sum_{k_1} \epsilon_{k_1} + \frac{N}{2} (K_S \Delta_{0x}^2 + K_H \Delta_{0z}^2), \tag{2.19}$$

where

$$\epsilon_{k_1} = \sqrt{2(t_0^2 + \alpha_S^2 \Delta_{0x}^2) + 2(t_0^2 - \alpha_S^2 \Delta_{0x}^2)\cos(2k_1 a) + \alpha_H^2 \Delta_{0z}^2}. \tag{2.20}$$

Eq. (2.19) is plotted for different situations in Figs. (2.7), (2.8) and (2.9). These figures can be understood analytically by expanding k_1 in Eq. (2.20) around $\pm\pi/2a$. Then, Eq. (2.19) becomes

$$E[\Delta_{0x}, \Delta_{0z}] \approx -\sum_{q_1} \sqrt{4a^2 t_0^2 q_1^2 + 4\alpha_S^2 \Delta_{0x}^2 + \alpha_H^2 \Delta_{0z}^2} + \frac{N}{2} (K_S \Delta_{0x}^2 + K_H \Delta_{0z}^2). \tag{2.21}$$

Therefore, the conditions $\partial E/\partial \Delta_{0x} = \partial E/\partial \Delta_{0z} = 0$ give

$$\left(\sum_{q_1} \frac{1}{\sqrt{4a^2 t_0^2 q_1^2 + 4\alpha_S^2 \Delta_{0x}^2 + \alpha_H^2 \Delta_{0z}^2}} - \frac{N}{2} \tilde{K}_S \right) \Delta_{0x} = 0,$$
$$\left(\sum_{q_1} \frac{1}{\sqrt{4a^2 t_0^2 q_1^2 + 4\alpha_S^2 \Delta_{0x}^2 + \alpha_H^2 \Delta_{0z}^2}} - \frac{N}{2} \tilde{K}_H \right) \Delta_{0z} = 0, \tag{2.22}$$

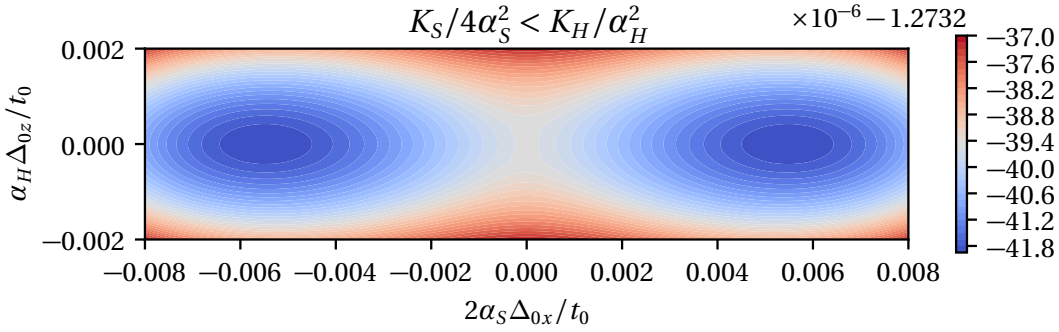

Figure 2.7
Plotting of E/t_0N for $\tilde{K}_S < \tilde{K}_H$. The mean-field order parameter minimizing the energy is $\left(\pm\frac{2at_0\Lambda}{\alpha_S}e^{-2\pi t_0\tilde{K}_S}, 0\right)$. We take $t_0\tilde{K}_S = 2$, $t_0\tilde{K}_H = 4$.

where $\tilde{K}_S = K_S/4\alpha_S^2$ and $\tilde{K}_H = K_H/\alpha_H^2$. Solving Eq. (2.22), the mean field order parameter is

$$
\begin{aligned}
(\Delta_{0x}, \Delta_{0z}) &= \left(\pm\frac{2at_0\Lambda}{\alpha_S}e^{-2\pi t_0\tilde{K}_S}, 0\right) \text{ for } \tilde{K}_S < \tilde{K}_H \\
(\Delta_{0x}, \Delta_{0z}) &= \left(0, \pm\frac{4at_0\Lambda}{\alpha_H}e^{-2\pi t_0\tilde{K}_H}\right) \text{ for } \tilde{K}_S > \tilde{K}_H \\
(\Delta_{0x}, \Delta_{0z}) &= 4at_0\Lambda e^{-2\pi t_0\tilde{K}_H}\left(\frac{1}{2\alpha_S}\sin\phi, \frac{1}{\alpha_H}\cos\phi\right) \text{ for } \tilde{K}_S = \tilde{K}_H.
\end{aligned}
\tag{2.23}
$$

In the third line of Eq. (2.23), the value of ϕ can be arbitrary because the ground state energy does not depend on it. In summary: (1) when $\tilde{K}_S < \tilde{K}_H$, the ground state displays SSH-like (bond density wave) order parameter; (2) when $\tilde{K}_S > \tilde{K}_H$, the ground state displays Holstein-like (site density wave) order parameter; (3) when $\tilde{K}_S = \tilde{K}_H$, there are a infinite number of sites with degenerate energy, therefore there would be a Goldstone mode know as "phason" [42].

The preceding observations are based on the mean-field approximation. It turns out that the zero-temperature phase diagram of Eq. (2.17) has been obtained in Ref. [17] using quantum Monte Carlo (see Fig. 2.10), which works well at large frequency. Depending on the value of parameters $\lambda_s \equiv \alpha_H^2/(K_H t_0)$ and $\lambda_b \equiv \alpha_S^2/(K_S t_0)$, there are three different phases: the SSH phase, the Holstein phase and the Luther-Emery metallic phase. When the values of the order parameters λ_b and λ_s increase the Luther-Emery metallic phase tends to vanish and there is a common boundary between the SSH and Holstein phases. The SSH CDW and Holstein CDW appear in the expected region. This is the region of the phase diagram where our mean-field treatment matches well the Monte Carlo prediction.

In order to realize a topological analogue of the magnetic bit, we place ourselves in the regime $\tilde{K}_S < \tilde{K}_H$. Then, we notice that Fig. (2.7) looks similar to that of a two-dimensional ferromagnet with easy-axis anisotropy. In our analogue, the two preferred

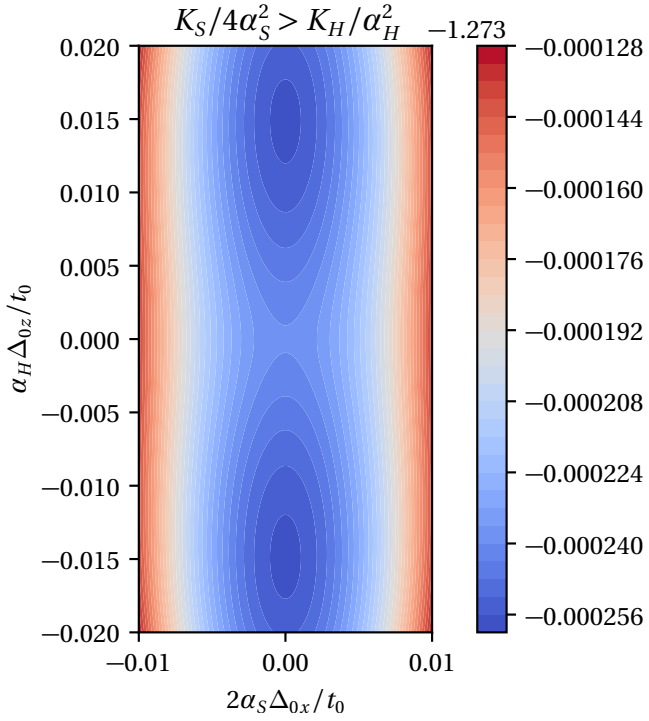

Figure 2.8
Plotting of E/t_0N for $\tilde{K}_S > \tilde{K}_H$. The mean-field order parameter minimizing the energy is $\left(0, \pm\frac{4at_0\Lambda}{\alpha_H}e^{-2\pi t_0\tilde{K}_H}\right)$. We take $t_0\tilde{K}_S = 4$, $t_0\tilde{K_H} = 2$.

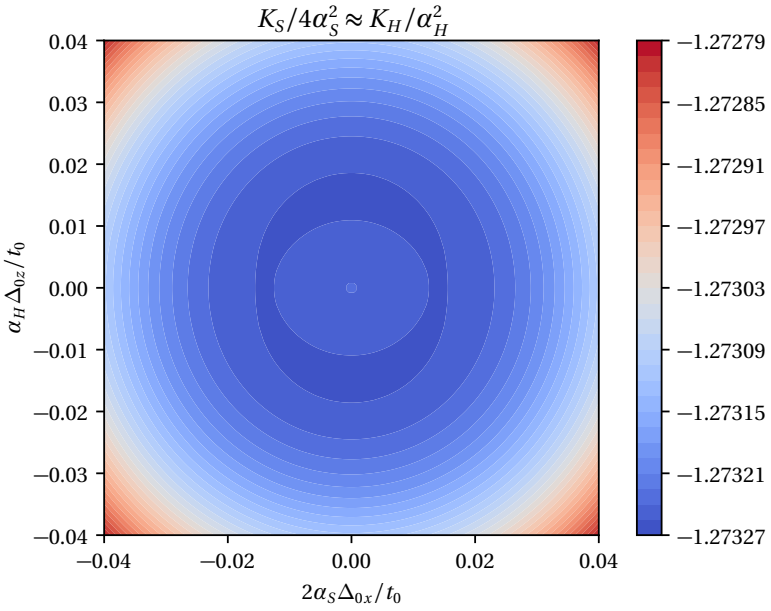

Figure 2.9
Plotting of E/t_0N for $\tilde{K}_S \approx \tilde{K}_H$. The mean-field order parameter minimizing the energy is $(\Delta_{0x}, \Delta_{0z}) = 4at_0\Lambda e^{-2\pi t_0\tilde{K}_H}\left(\frac{1}{2\alpha_S}\sin\phi, \frac{1}{\alpha_H}\cos\phi\right)$. We take $t_0\tilde{K}_S = 1.7$, $t_0\tilde{K}_H = 2$. The Goldstone mode does not appear in the case $\tilde{K}_S \approx \tilde{K}_H$ but instead appears when $\tilde{K}_S \approx \tilde{K}_H$, this is because the graph is not given by expanding k_1 around $\pm\pi/2a$, but is given by direct calculation of Eq. (2.19).

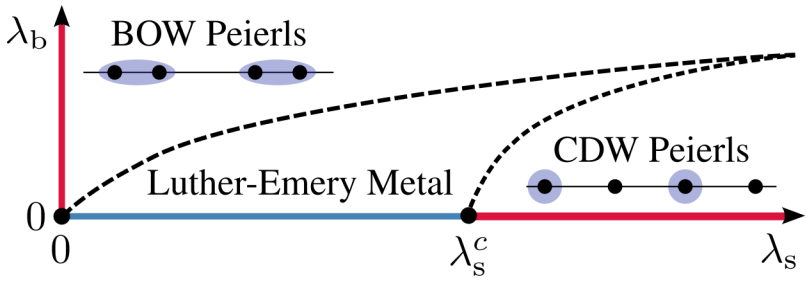

Figure 2.10
Phase diagram for SSH-Holstein model, where $\lambda_b \equiv \alpha_S^2/(K_S t_0)$, $\lambda_s \equiv \alpha_H^2/(K_H t_0)$, $K_S = m_S\omega_S^2$ and $K_H = m_H\omega_H^2$. Dashed lines are the phase boundaries. Figure taken from Ref. [17].

(anti-parallel) orientations of the magnetization can be mapped to the order parameters Δ_{0x} and $-\Delta_{0x}$. For the case $\tilde{K}_S = \tilde{K}_H$ (see Fig (2.9)), the analouge of the magnetic anisotropy energy vanishes and the magnetization has no preferred direction. In this case, the rotational symmetry is spontaneously broken in the ground state, and the low-energy excitation is a gapless magnon; such situation is clearly not desirable for a magnetic bit.

The dynamics of the magnetization in a magnetic material is described by Landau-Lifshitz-Gilbert equation [8], which is a ground state non-linear differential equation beyond the small perturbations of the angle. Is there a similar non-perturbative equation for describing the change in the band topology? This is the main question we will address in the following chapters.

Chapter 3

Small-angle order parameter dynamics of the SSH-Holstein model

Thus far we have discussed the mean-field ground state of the SSH-Holstein model and we have described the presence of the two topologically distinct ground states therein. In this chapter, we determine the dynamics of small fluctuations around the mean-field ground state (small-angle dynamics). While insufficient to describe a topological bit, the calculations of this chapter set the notation and formalism for Chapter 4, which will concentrate on the large-angle dynamics of the order parameter.

3.1 Continuum model

We begin by introducing a continuum model, which will facilitate the calculations that follow below. The continuum model is motivated by the fact that, for half-filling, low energy excitations are concentrated in the vicinity of $k_1 = \pm\pi/2a$ [14]. This allows to write

$$\begin{aligned} c_j &= \sum_{k_1} \frac{1}{\sqrt{N}} \Psi(k_1) e^{-ik_1 x} = \sum_{k_1 \approx -k_F} \frac{1}{\sqrt{N}} \Psi(k_1) e^{-ik_1 x} + \sum_{k_1 \approx k_F} \frac{1}{\sqrt{N}} \Psi(k_1) e^{-ik_1 x} \\ &= \frac{1}{\sqrt{a}} \left(\Psi_L(x) e^{ik_F x} + \Psi_R(x) e^{-ik_F x} \right), \end{aligned} \tag{3.1}$$

and

$$\Psi_{R,L} = \sqrt{Na} \int_{-\lambda}^{\lambda} \frac{dk}{2\pi} \Psi_{k \pm K_F} e^{-ikx}, \tag{3.2}$$

where Ψ_L is the field operator for the left-moving fermions, Ψ_R is the field operator for the right-moving fermions and $k_F = \pi/2a$. Substituting Eq. (3.1) into Eq. (2.17) and

ignoring $\exp[\pm i2k_F x]$ since it is fast-varying, then the Hamiltonian of the SSH-Holstein model becomes

$$H = \int dx \Psi^\dagger h \Psi + \frac{1}{2a} m_S \int dx \Big[\dot{\Delta}_x^2 + \omega_S^2 \Delta_x^2\Big] + \frac{1}{2a} m_H \int dx \Big[\dot{\Delta}_z^2 + \omega_H^2 \Delta_z^2\Big], \tag{3.3}$$

where $\Psi = (\Psi_L, \Psi_R)$ and

$$h = -iv\sigma^z \partial_x - 2\alpha_s \Delta_x \sigma^y + \alpha_H \Delta_z \sigma^x \tag{3.4}$$

is the Hamiltonian of 1D Dirac fermions with dynamical masses and velocity $v = 2at_0$. If we define

$$\begin{aligned} -2\alpha_S \Delta_x &\equiv \Delta \sin\phi \\ \alpha_H \Delta_z &\equiv \Delta \cos\phi, \end{aligned} \tag{3.5}$$

then h is consistent with the low-energy effective Hamiltonian derived by Goldstone and Wilczek [15] for an incommensurate charge density wave (ICDW). The ICDW is a charge density wave with degenerated ground state energy, consequently, there will be a goldstone mode known as "phason", which indicates that the CDW is sliding. However, in their paper, they treat Δ and ϕ as known parameters, but in this project we want to unveil their dynamics.

3.2 Perturbations

In order to study the dynamics of the order parameter, it is important to include the effect of external perturbations. In the presence of such perturbations, Eq. (3.4) gets an additional term that we label as δH. In the low-energy subspace of R and L fermions, a generic perturbation can be written as

$$\delta H = \int dx \Psi^\dagger \delta h \Psi = \int dx \Psi^\dagger (\mathbf{B}\cdot\boldsymbol{\sigma} + B_0 \mathrm{I}) \Psi, \tag{3.6}$$

where I is the identity matrix, and $\boldsymbol{\sigma}$ is a vector of Pauli matrices in the (L,R) space. Let us discuss the physical meaning of the different components of the perturbations $(B_x, B_y, B_z) = \mathbf{B}$ and B_0. To begin with, we consider a spatial modulation of the onsite potential,

$$\delta H = \sum_j V_j c_j^\dagger c_j. \tag{3.7}$$

Using Eq. (3.1) and transferring $V(x)$ to Fourier space as $V(x) = \sum_{k_1} v_{k_1} e^{ik_1 x}$, we get

$$\begin{aligned} \delta H &\propto \int dx \Psi^\dagger [v_0 I + \Re(v_{2k_F})\sigma^x - \Im(V_{2k_F})\sigma^y]\Psi \\ &= \int dx \Psi^\dagger [v_0 I + B_x \sigma^x + B_y \sigma^y]\Psi, \end{aligned} \tag{3.8}$$

where v_0 renormalizes the chemical potential. Thus, a modulation of the onsite potential produces the perturbation B_x and B_y. If the modulation is symmetric in space ($V(x) = V(-x)$), then only B_x is present. Next, we consider the effect of a modulated strain:

$$\delta H = \sum_j V_j (c_j^\dagger c_{j+1} + H.c.), \tag{3.9}$$

which leads to

$$\delta H \propto \int dx \Psi^\dagger [2\Re(v_{2k_F})\sigma^y]\Psi = \int dx \Psi^\dagger [B_y \sigma^y]\Psi. \tag{3.10}$$

Thus a modulation of strain produces nonzero B_y. Finally, B_0 and B_z can be interpreted as scalar and vector electromagnetic potentials, respectively, because B_0 couples to the charge density and B_z enters the Hamiltonian as $(-iv\partial_x + B_z)\sigma^z$.

3.3 Effective action for the order parameters

A convenient and standard way to compute the order parameter dynamics is through the minimization of an effective action. To obtain such an effective action, we begin by writing the partition function of the system in the imaginary-time path integral formalism [3]:

$$Z = \int D(\Psi^\dagger, \Psi, \Delta_x, \Delta_z)\, e^{-S[\Psi^\dagger, \Psi, \Delta_x, \Delta_z]}, \tag{3.11}$$

where

$$S\left[\Psi^\dagger, \Psi, \Delta_x, \Delta_z\right] = \int d\tau dx \left[\Psi^\dagger \partial_\tau \Psi - \mu \Psi^\dagger \Psi\right] + \int d\tau\, (H + \delta H) \tag{3.12}$$

is the action of the system, μ is the chemical potential, and $\tau = it$ is the imaginary time. The full action in Eq. (3.12) contains both fermion and phonon (order parameter) fields. However, we are interested only in the dynamics of the order parameters.

One benefit of using the path-integral formalism is that we can integrate out the electronic degrees of freedom ($\Psi^\dagger$, Ψ) in order to quantify their influence in the dynamics of the order parameter (Δ_x, Δ_z). Because Eq. (3.12) is quadratic in the fermion fields, the integration of the electronic fields can be done exactly using the well-known formula [3]

$$\begin{aligned} \int D[\Psi^\dagger, \Psi, \Delta_x, \Delta_y] e^{-\int d\tau dx \Psi^\dagger G^{-1} \Psi} &= \int D[\Delta_x, \Delta_y] \det(G^{-1}) \\ &= \int D[\Delta_x, \Delta_y] \exp[\mathrm{Tr} \ln G^{-1}], \end{aligned} \tag{3.13}$$

where $G^{-1} = \partial_\tau - \mu + h + \delta h$, and Tr represents the trace over both space-time and the (L,R) pseudospin. In the usual jargon, G is the electronic Green's function. As a result, the partition function reads

$$Z = \int D[\Delta_x, \Delta_z] e^{-S_{\text{eff}}(\Delta_x, \Delta_z)}, \tag{3.14}$$

where $S_{\text{eff}} = S_{\text{ph}} - \text{Tr} \ln G^{-1}$ is the so-called effective action for the order parameters, and

$$S_{\text{ph}} = \int d\tau dx \left(\frac{1}{2a} m_S \left[\dot{\Delta}_x^2 + \omega_S^2 \Delta_x^2 \right] + \frac{1}{2a} m_H \left[\dot{\Delta}_z^2 + \omega_H^2 \Delta_z^2 \right] \right) \tag{3.15}$$

is the phonon-only part of the effective action. From the effective action, we obtain the dynamics of the order parameters in two steps: first, we minimize the effective action via $\delta S_{\text{eff}} / \delta \mathbf{\Delta} = 0$, and afterwards we switch back to real time. There is a problem, however. While the expression for S_{eff} is exact in principle, in practice it cannot be computed exactly because G^{-1} contains order parameter fields with arbitrary time and space dependence. As a result, we are unable to compute the trace over space and time. Thus, it is necessary to resort to approximations. The simplest approximation one can think of is to assume that the external fields are weak and that the deviations of the order parameters from their mean-field values are small. Then, one can write

$$(\Delta_x, \Delta_z) = (\Delta_{0x} + \delta\Delta_x, \Delta_{0z} + \delta\Delta_z), \tag{3.16}$$

where the first and second terms in the right hand side describe the mean-fields and the small fluctuations, respectively. As stated in Chapter 2, we choose the microscopic parameters of the Hamiltonian such that $\Delta_{0z} = 0$. Therefore, $G^{-1} = G_0^{-1} + V$, where

$$G_0^{-1} = \partial_\tau - iv\sigma^z \partial_x - \mu - 2\alpha_S \Delta_{0x} \sigma^y \tag{3.17}$$

is the mean-field part of the electronic Green function and

$$V = G^{-1} - G_0^{-1} = -2\alpha_S \delta\Delta_x \sigma^y + \alpha_H \delta\Delta_z \sigma^x + \delta h \tag{3.18}$$

is the perturbation that is assumed to be "small". Now the effective action can be written as

$$S_{\text{eff}} = S_{\text{ph}} - \text{Tr}\left[G_0^{-1} \right] + \sum_n S_n, \tag{3.19}$$

where

$$S_n = \frac{1}{n} \text{Tr}\left[(G_0 V)^n \right] \tag{3.20}$$

and we have used

$$\text{Tr}[\ln G^{-1}] = \text{Tr} \ln[G_0^{-1}] + \text{Tr} \ln(1 - G_0 V). \tag{3.21}$$

From now on we truncate the perturbative expansion of the effective action at $n = 2$. Accordingly, the angle $\phi = \arctan(-2\alpha_S \Delta_x / \alpha_H \Delta_z)$ introduced in Eq. (3.5) will be restricted to the vicinity of $\pi/2$ or $-\pi/2$, depending on the sign of Δ_{0x}. It is in this sense that the dynamics of the order parameter can be called "small-angle dynamics".

3.4 First order expansion of the action

Let us calculate the terms in the effective action that are linear in the fluctuations and in the external perturbations. We begin concentrating on $\mathrm{Tr}[G_0 V]$. Since the trace is basis-independent, we choose to write it in frequency and momentum space (ω_n, k_1). The motivation for this choice is that G_0 is diagonal in frequency and momentum space, as the mean-field ground state is static and spatially uniform. Inverting Eq. (3.17) we obtain

$$G_0(\omega_n, k_1) = \frac{i\omega_n + \mu + 2at_0 k_1 \sigma^z - 2\alpha_S \Delta_{0x}\sigma^y}{(i\omega_n + \mu)^2 - \epsilon_{k_1}^2}, \tag{3.22}$$

where

$$\epsilon_{k_1} = \sqrt{v^2 k_1^2 + 4\alpha_S^2 \Delta_{0x}^2} \tag{3.23}$$

is the excitation energy for 1D massive Dirac fermions, $\omega_n = (2n+1)\pi k_B T$ is the fermionic Matsubara frequency, T is the temperature, k_B is the Boltzmann constant,

$$V(q) = -2\alpha_S \sigma^y \delta\Delta_x(q) + \alpha_H \sigma^x \delta\Delta_z(q) + \mathbf{B}(q)\cdot\boldsymbol{\sigma} + B_0(q)\mathrm{I} \tag{3.24}$$

is the perturbation in Fourier space, and $q = (q_0, q_1) = (\omega_n - \omega_n', k_1 - k_1')$. We use the following convention for Fourier transforms:

$$\begin{aligned}\Psi(x,\tau) &= \frac{1}{\sqrt{\beta N a}} \sum_{\omega_n, k_1} \exp(-i\omega_n \tau)\exp(-ik_1 x_1)\Psi(k_1, \omega_n) \\ \Psi(\omega_n, k_1) &= \frac{1}{\sqrt{N a \beta}} \int dx d\tau \exp(i\omega_n \tau)\exp(ik_1 x)\Psi(x,\tau).\end{aligned} \tag{3.25}$$

Using these conventions, writing $k = (\omega_n, k_1)$ and defining "tr" for the trace over (L,R) pseudospin, we have

$$\begin{aligned}\mathrm{Tr}[G_0 V] &= \sum_k \mathrm{tr}\langle k|G_0 V|k\rangle = \sum_k \mathrm{tr}\, G_0(k)\langle k|V|k\rangle = \frac{1}{\sqrt{\beta N a}}\sum_k \mathrm{tr}\, G_0(k) V(0) \\ &= -\big(B_y(0) - 4\alpha_S^2 \Delta_{0x}\delta\Delta_x(0)\big)\frac{1}{\sqrt{\beta N a}}\sum_{\omega_n}\sum_{k_1}\frac{1}{(i\omega_n+\mu)^2 - \epsilon_{k_1}^2},\end{aligned} \tag{3.26}$$

where we have used the notation

$$\langle k|V|k'\rangle = \frac{1}{\sqrt{\beta N a}} V(k'-k), \tag{3.27}$$

valid because V is local in space and time. The next step is to compute the momentum and frequency sums in Eq. (3.26). We begin with the sum of Matsubara frequencies, which can be done as explained in Ref. [3]:

$$\frac{1}{\beta}\sum_{\omega_n}\frac{1}{(i\omega_n+\mu)^2 - \epsilon_{k_1}^2} = -\frac{1}{\beta}\sum_\lambda \mathrm{Res}\left[\frac{1}{(z+\mu)^2 - \epsilon_{k_1}^2}\right]\frac{\beta}{\exp(\beta z)+1}\Big|_{z=z_\lambda} = \frac{f_{k_1,-} - f_{k_1,+}}{2\epsilon_{k_1}},$$

where λ is an index denoting poles, $z = i\omega_n$, "+" represents the upper electron band and "−" represents the lower electron band, as indicated in Fig. (2.2), and $f_{k_1,\pm} = 1/\left[\exp(-\beta(\pm\epsilon_{k_1} - \mu) + 1\right]$ is the Fermi-Dirac distribution function. We will be interested in the low-temperature regime, where $f_{k_1,+} \approx 0$ and $f_{k_1,-} \approx 1$. Accordingly,

$$S_1 = \left(B_y(0) - 4\alpha_S^2 \Delta_{0x} \delta\Delta_x(0)\right) \sum_{k_1} \frac{1}{2\epsilon_{k_1}} + K_S \Delta_{0x} \delta\Delta_x(0). \tag{3.28}$$

The first term of Eq. (3.28) does not contribute to the equation of motion $\delta S_{\text{eff}}/\delta\mathbf{\Delta} = 0$ because it is independent from $\delta\Delta_x$ and $\delta\Delta_z$. The second term does not contribute either because time average of the fluctuation is zero.

3.5 Second order expansion of the action

Now we calculate the terms in the effective action which are quadratic in the perturbation V. We will use the well-known formula [3, 32]

$$\text{Tr}[G_0 V G_0 V] = \frac{1}{\beta N a} \sum_{q_1,q_0} \frac{1}{Na} \sum_{k_1,n,n'} |\langle k_1 n|V|k_1 + q_1 n'\rangle|^2 \frac{f_{k_1,n} - f_{k_1+q_1,n'}}{\epsilon_{k_1,n} - \epsilon_{k_1+q_1,n'} + iq_0}, \tag{3.29}$$

where $n = \pm$ and $n' = \pm$ are the mean-field electronic band indices, $\epsilon_{k_1\pm} = \pm\epsilon_{k_1}$ is the band energy, $|k_1, +\rangle = (\cos(\theta_{k_1}/2), \sin(\theta_{k_1}/2))^T$ and $|k_1, -\rangle = (-\sin(\theta_{k_1}/2), \cos(\theta_{k_1}/2))^T$ are the band eigenstates, and $\cos\theta_{k_1} = 2vk_1/\epsilon_{k_1}$. At zero temperature, only $n = -n'$ contribute to Eq. (3.29). Therefore the only matrix elements to compute are

$$\begin{aligned}|\langle k_1, +|V|k_1', -\rangle|^2 = {} & 4\alpha_S^2 \cos^2\left(\frac{\theta_{k_1} + \theta_{k_1'}}{2}\right) |\delta\tilde{\Delta}_x(q)|^2 + \alpha_H^2 \cos^2\left(\frac{\theta_{k_1} - \theta_{k_1'}}{2}\right) |\delta\tilde{\Delta}_z(q)|^2 \\ & - 2i\alpha_S\alpha_H \cos\left(\frac{\theta_{k_1} + \theta_{k_1'}}{2}\right) \cos\left(\frac{\theta_{k_1} - \theta_{k_1'}}{2}\right) \left[\delta\tilde{\Delta}_x^\star(q)\delta\tilde{\Delta}_z(q) - H.c\right]\end{aligned} \tag{3.30}$$

and

$$|\langle k_1, -|V|k_1', +\rangle|^2 = |\langle k_1, +|V|k_1', -\rangle|^2_{\alpha_H \to -\alpha_H}, \tag{3.31}$$

where we have defined $\delta\tilde{\Delta}_z \equiv \delta\Delta_z + B_x/\alpha_H$ and $\delta\tilde{\Delta}_x \equiv \delta\Delta_x - B_y/2\alpha_S$. In Eq. (3.30), we have omitted the gauge fields B_0 and B_z for simplicity. We will treat them in the next chapter.

Using Eq. (3.29) we get

$$S_2 + S_{\text{ph}} = \frac{1}{2\beta L} \sum_{q_0,q_1} (\delta\tilde{\Delta}_x^\star, \delta\tilde{\Delta}_z^\star) K (\delta\tilde{\Delta}_x, \delta\tilde{\Delta}_z)^T, \tag{3.32}$$

where K is a 22 matrix. In the long wavelength and the low energy approximation, i.e. $|q_0|, v|q_1| \ll |\Delta_{0x}|$, the matrix elements of K are

$$\begin{aligned}
K_{00}(q) &\approx \frac{1}{N}\frac{\partial^2 E}{\partial \Delta_x^2}\bigg|_{(\Delta_{x0},0)} + \frac{\alpha_S^2}{24\pi t_0}\frac{v^2 q_1^2 + q_0^2}{\alpha_S^2 \Delta_{0x}^2} + m_S^2 q_0^2, \\
K_{01}(q) &\approx \frac{\alpha_S \alpha_H}{16\pi^3}\frac{a q_1 q_0}{t_0^2} = -K_{10}, \\
K_{11}(q) &= \frac{1}{N}\frac{\partial^2 E}{\partial \Delta_z^2}\bigg|_{(\Delta_{x0},0)} + \frac{\alpha_H^2}{32\pi t_0}\frac{v^2 q_1^2 + q_0^2}{\alpha_S^2 \Delta_{0x}^2} + m_H^2 q_0^2.
\end{aligned} \tag{3.33}$$

In the static and uniform configuration ($q_0, q_1 = 0$), K behaves as a matrix of spring constants,

$$\begin{aligned}
K_{00}(0) &= \frac{1}{N}\frac{\partial^2 E}{\partial \Delta_x^2}\bigg|_{(\Delta_{x0},0)} \\
K_{11}(0) &= \frac{1}{N}\frac{\partial^2 E}{\partial \Delta_z^2}\bigg|_{(\Delta_{x0},0)} \\
K_{01}(0) &= -K_{10} = 0.
\end{aligned} \tag{3.34}$$

From Eq. (3.32) we obtain the equation of motion

$$\begin{bmatrix} K_{00} & K_{01} \\ K_{10} & K_{11} \end{bmatrix} \begin{bmatrix} \delta\tilde{\Delta}_x \\ \delta\tilde{\Delta}_z \end{bmatrix} = 0. \tag{3.35}$$

Considering the spatially uniform dynamics, Eq. (3.35) can be rewritten as

$$\begin{aligned}
K_{00}(0)\delta\Delta_x + \left(\frac{1}{24\pi t_0 \Delta_{0x}^2} + m_S\right)\partial_t^2 \delta\Delta_x &= K_{00}(0)\frac{B_y}{2\alpha_S} + \left(\frac{1}{24\pi t_0 \Delta_{0x}^2} + m_S\right)\frac{\partial_t^2 B_y}{2\alpha_S} \\
K_{11}(0)\delta\Delta_z + \left(\frac{\alpha_H^2}{32\pi t_0 \alpha_S^2 \Delta_{0x}^2} + m_H\right)\partial_t^2 \delta\Delta_z &= -K_{11}(0)\frac{B_y}{\alpha_H} - \left(\frac{1}{32\pi t_0 \Delta_{0x}^2} + m_H\right)\frac{\partial_t^2 B_y}{\alpha_H}.
\end{aligned} \tag{3.36}$$

These equations describe harmonic oscillations around the local minimum $(\Delta_{0x}, 0)$ with external forces. When $B_y = 0 = B_x$ the dispersion relation for the low energy fluctuations of the order parameter can be obtained by equaling the determinant of the matrix in Eq (3.35) to zero.

This concludes our discussion of small-angle order parameter dynamics. We will not discuss further aspects of small-angle dynamics (such as collective modes), since the main goal of the present chapter is to set the technical formalism for the next chapter. Next, we will go beyond small-angle order parameter dynamics by a more judicious choice of perturbation. That will allow us to realize a proof-of-principle for the topological bit.

Chapter 4

Large-angle order parameter dynamics of the SSH-Holstein model

In the previous chapter, we studied the small-angle order parameter dynamics of the SSH-Holstein model. In the SSH-Holstein model, the charge-density wave order parameter can be written as $\Delta(\sin\phi, \cos\phi, 0)$, where ϕ is the order parameter angle and Δ is the amplitude. In Chapter 3 we studied the small-angle order parameter dynamics (ϕ close to $\pi/2$ or $-\pi/2$). However, in order to describe the dynamics across a topological phase transition, we need an equation of motion for the order parameter that will be valid for an arbitrary value of ϕ ("large angle" dynamics). The purpose of the present chapter is to introduce a method that fulfills that need and enable us to provide a proof-of-principle for the topological analogue of the magnetic bit. We have since aware of similar transformation in the literature of incommensurate charge density waves (ICDW) [15, 34, 41, 24].

In Sec. 4.1 we will introduce the method of calculation. In Sec. 4.2 we will calculate the order parameter as a function of the order parameter angle, and will derive the analogue of the magnetic anisotropy energy in our system. In Sec. 4.3 we will derive the chiral anomaly using Fujikawa method. In Sec. .4 we will calculate the contribution to the action from the regular part. In Sec. 4.5 and Sec. 4.6 we will list and solve some problems during the calculations. In Sec. 4.7 we will compare our result to earlier works [15, 34, 41, 24]. In Sec. 4.8 we will discuss the physical meaning of the anomaly term. In Sec. 4.8 we will derive the equation of motion for the order parameter involving a damping term. In Sec. 4.9 we will discuss the similarity with the Josephson effect. In Sec. 4.10 we will discuss the polarization. In Sec. 4.11 we will discuss the shape of the pulse which could induce the topological phase transition.

4.1 Chiral gauge transformation

In chapter 3, we presented a method to calculated the effective action of the order parameter and the equation of motion in the presence of external perturbations. Then, we performed perturbation theory in the vicinity of the ground state. As a result, the order parameter angle ϕ was always limited to the neighborhood of $\pm\pi/2$. In this section, using the same overall method we will introduce a gauge transformation of the coordinate which will allow us to study the same system, but in the large angular fluctuation regime.

Let us begin by recalling the electronic part of the action, obtained in Chapter 3:

$$S_{\text{ele}} = \int dx d\tau \Psi^\dagger [\partial_\tau - iv\sigma^z \partial_x - \Delta\boldsymbol{\Omega}\cdot\boldsymbol{\sigma} - \mu + \mathbf{B}\cdot\boldsymbol{\sigma} + B_0 I]\Psi, \tag{4.1}$$

where $\Omega = (\cos\phi, \sin\phi, 0)$ and ϕ is defined in Eq. (3.5). Now consider a change of variables $\Psi' = R\Psi$, where $R = \exp(-i\sigma_z\phi/2)$ is a unitary operator that rotates the left-moving and right-moving fermions in the *opposite* sense by an angle $\pi/2$. Because of this twisted sense of rotation, R can be called a chiral gauge transformation. Upon this transformation, the electronic action becomes

$$\begin{aligned} S_{\text{ele}} = \int dx d\tau \Psi'^\dagger \Big[&\partial_\tau - iv\sigma^z\partial_x + \Delta\sigma^x - \frac{i}{2}\sigma^z\partial_\tau\phi - \frac{v}{2}\partial_x\phi \\ &- \mu + \sigma^x(\mathbf{B}\cdot\boldsymbol{\Omega}) - \sigma^y[(\mathbf{B}\times\boldsymbol{\Omega})\cdot\hat{\mathbf{z}}] + B_z\sigma^z + B_0 I \Big]\Psi'. \end{aligned} \tag{4.2}$$

Here, we notice that the time and space gradients of ϕ have been separated out from ϕ itself. The later only appears only in terms that multiply with the small external perturbation $\mathbf{B}$. Thus, this opens the door of doing perturbation theory in $\partial_\tau\phi$ and $\partial_x\phi$ instead of ϕ itself.

4.2 Magnitude of the order parameter and anisotropy energy

In Eq. (4.2) there remains a difficulty in the term $\Delta\sigma^x$. Because Δ is generally space and time dependent, the calculation of the effective action for the order parameter becomes very complicated. To overcome this difficulty, we borrow an approximation method from magnetism, for temperatures below the Curie temperature, the fluctuations in the magnitude of the magnetization are neglected because they involve higher energies than the fluctuations in the angle of the magnetization. In our model, the magnetization could be mapped to the magnitude Δ of the charge density wave order parameter. Then, we assume that Δ can be minimizing the total energy of the system for each value of ϕ. This amounts to neglecting the fluctuations of Δ around its mean-field value. Ignoring the contributions of $\mathbf{B}$, the total energy of the system is given by Eq. (2.19). In the continuum approximation (cf. Chapter 3), the sum over the wave vector can be done analytically as function of Δ and ϕ (which are treated as parameters in calculation).

The price of the analytical convenience of the continuum model is the need to introduce an ultraviolet (UV) momentum cutoff Λ. Once we have obtained the energy $E[\Delta, \phi]$, we minimize it with respect to Δ. Such minimization gives

$$\Delta_{\min} = 4at_0\Lambda \exp(-2\pi t_0(\tilde{K}_S \sin^2\phi + \tilde{K}_H \cos^2\phi)). \tag{4.3}$$

We can define a parameter γ that

$$\gamma = \frac{\Delta_0^2}{2a}(\tilde{K}_S - \tilde{K}_H). \tag{4.4}$$

If $\tilde{K}_H = \tilde{K}_S$, the magnitude of order parameter is

$$\Delta_0 = 4at_0\Lambda \exp(-2\pi t_0 \tilde{K}_H), \tag{4.5}$$

we will assume that $\tilde{K}_S, \tilde{K}_H$ are close to each other, so that

$$\Delta_{min} = \xi \cos 2\phi - \xi + \Delta_0, \tag{4.6}$$

where ξ is defined as

$$\xi = \pi t_0 \Delta_0 (\tilde{K}_S - \tilde{K}_H). \tag{4.7}$$

We will treat ξ as pertubation, which represents a first order dependence on the magnitude of order parameter.

Now we find the expression of the minimum energy (ground state energy) by substituting the minimized order parameter Δ_{min} in Eq. (2.19):

$$\begin{aligned} E_{min} = \log \frac{4at_0\Lambda\Delta_{min}}{16a^2t_0^2\Lambda^2 + \Delta_{min}^2} &\approx \log \frac{\Delta_{min}}{4at_0\Lambda} \\ &= \log(e^{-2\pi t_0(\tilde{K}_s \sin^2\phi + \tilde{K}_H \cos^2\phi)}) \\ &= -2\pi t_0 \left[\left(\tilde{K}_S - \tilde{K}_H\right)\sin^2\phi + \tilde{K}_H\right], \end{aligned} \tag{4.8}$$

thus

$$E_{min}[\phi] \approx -\frac{N\Delta_{min}^2(\phi)}{8\pi t_0}, \tag{4.9}$$

and

$$\frac{\partial E_{min}}{\partial \phi} = 0 \rightarrow \gamma \sin 2\phi = 0, \tag{4.10}$$

For $\gamma < 0$, the energy of the system reaches a local minimum at $\phi = \frac{\pi}{2}(2n+1)$, and reaches a local maximum at $\phi = n\pi$, where n is an integer.

4.3 The chiral anomaly

In section 4.1, we have seen how the electronic action changes under a chiral gauge transformation. This is not the whole story. In 1979, Kazuo Fujikawa [12, 13] pointed out that, when a chiral gauge transformation is applied to Dirac fermions in even space-time dimensions, the measure of the path integral changes as well. This change in the measure results in an additional term in the effective action, which is known as the chiral anomaly contribution. In this section, we calculate the anomaly contribution appearing in our model. We denote the anomaly part of the action as S_a.

Including the electromagnetic vector potential $A = (A_0, A_1)$, the electronic part of the action of the system can be written as [38]

$$S_{\text{ele}} = -i \int d\tau dx \bar{\Psi} \left[i\tilde{\not{D}} + iM(\phi) \right] \Psi, \tag{4.11}$$

where

$$\bar{\Psi} = \Psi^\dagger \sigma^x. \tag{4.12}$$

The Hermitian and gauge-invariant derivative operator $i\tilde{\not{D}}$ is

$$i\tilde{\not{D}} = i\not{\partial} + e\tilde{\not{A}}, \tag{4.13}$$

where $\tilde{\not{A}} = \tilde{A}_\mu \gamma^\mu$ is the "Feynman slashed notation", γ^μ are Dirac gamma matrices with $\mu = 0, 1$ ($\gamma^0 = \sigma^x, \gamma^1 = -\sigma^y$), which satisfy the anti-commutation relation $[\gamma^u, \gamma^v]_+ = 2\delta^{\mu\nu}$ (we take the Fermi velocity $v = 1$), and $\tilde{A}_0 = A_0 - i\frac{v}{2e}\partial_x \phi$ and $\tilde{A}_1 = A_1 + \frac{i}{2e}\partial_\tau \phi$ are the generalized gauge fields [29]. The chemical potential μ can be absorbed by A_0 and B_z can be absorbed by A_1. The mass of the fermion is

$$M(\phi) = -\Delta(x)\cos\phi + B_x - \sigma^z (B_y - \Delta(x)\sin\phi), \tag{4.14}$$

The general formula for the partition function is

$$Z = \int D[\Psi, \bar{\Psi}, \phi, \Delta] e^{-S[\Psi, \bar{\Psi}, \phi, \Delta]} = \int D[\bar{\Psi}', \Psi', \phi, \Delta] \exp[-2 \ln \mathrm{Tr} J] e^{-S[\Psi', \bar{\Psi}', \phi, \Delta]}, \tag{4.15}$$

where J is the Jacobian and it involves singularity. The crucial part of the Fujikawa method is the singularity should be regularized, details calculations are in Appendix A. The action for the chiral anomaly is

$$S_a = -2 \ln \mathrm{Tr} J = \frac{i}{2\pi} \int d\tau dx \Big[e\phi E_x + \frac{1}{4\pi v} (\partial_\tau \phi)^2 + \frac{v}{4\pi} (\partial_x \phi)^2 \Big], \tag{4.16}$$

the action for the chiral anomaly in the real time is

$$S_a = \frac{-1}{2\pi} \int dt dx \Big[e\phi E_x - \frac{1}{4\pi v} (\partial_t \phi)^2 + \frac{v}{4\pi} (\partial_x \phi)^2 \Big]. \tag{4.17}$$

At first glance, one may be concerned with the fact that S_a appears to change under $\phi \to \phi + 2\pi$. Yet, ϕ and $\phi + 2\pi$ should be physically indistinguishable. This implies that $\exp(-S_a)$, which appears directly in the partition function, must be invariant under ϕ to $\phi + 2\pi$. Fortunately, this turns out to be the case, as shown by the so-called Atiyah-Singer-Patodi index theorem [38].

The chiral anomaly action S_a has important physical consequences. Let us discuss a few of them. First, using Eq. (4.17), we notice that

$$\begin{aligned} j_0 &= \frac{\delta S}{\delta A^0} = -e\partial_x \phi = -\frac{1}{2} e\delta \\ j_1 &= \frac{\delta S}{\delta A^1} = \frac{1}{2} e\partial_t \phi . \end{aligned} \tag{4.18}$$

Therefore, space- and time-gradients of angle ϕ result in electric charge (j_0) and current densities (j_1). The factor of $1/2$ in Eq. (4.18) is indicative of charge fractionalization. For example, let us suppose a sharp domain wall between $\phi = \pi/2$ and $\phi = -\pi/2$, centered at $x = 0$. It follows from Eq. (4.18) that $j_0 = -1/2e\delta(x)$. Thus, a particle of charge $e/2$ is trapped at the domain wall between a topologically trivial and a topologically non-trivial insulator. The result in known in the SSH model literature, from an alternative point of view [28].

4.4 Perturbative contributions to the effective action

In the previous section, we derived the contribution to the effective action of the phonon order parameter, coming from the chiral gauge transformation. That contribution is non-perturbative. In this section, we integrate out electrons (like in Chapter 3) in order to obtain the remaining parts of the effective action. The starting point is the partition function:

$$Z \simeq \int D[\phi] e^{-S_a - S_{\text{ph}}} \det[G^{-1}(\tau, x)] = \int D[\phi] e^{-S_a - S_{\text{ph}}} \exp(\text{Tr}\ln[G^{-1}]), \tag{4.19}$$

where

$$\begin{aligned} G^{-1} = {} & \partial_\tau - iv\sigma^z \partial_x + \Delta_{min}\sigma^x + \sigma^x(\mathbf{B}\cdot\mathbf{\Omega}) - \sigma^y[(\mathbf{B}\times\mathbf{\Omega})\cdot z] + \sigma^z B_z - \mu + B_0 I \\ & - \frac{i}{2}\sigma^z \partial_\tau \phi - \frac{v}{2}\partial_x \phi - ev\sigma^z A_1 - ievA_0 \end{aligned} \tag{4.20}$$

is the inverse electronic Green function after the chiral gauge transformation. As mentioned in Chapter 3, we notice once again that the electromagnetic gauge fields A_1 and A_0 can be absorbed into the terms containing B_z and B_0. With this in mind, from here on we only keep A_0 and B_z.

We define the unperturbed inverse electronic Green function

$$G_0^{-1}(x, \tau) = \partial_\tau - iv\sigma^z \partial_x - \mu + \Delta_0 \sigma^x \tag{4.21}$$

and a perturbation

$$\begin{aligned} V(x,\tau) &= G_0^{-1} - G^{-1} \\ &= -\sigma^x(\mathbf{B}\cdot\mathbf{\Omega}) + \sigma^y[(\mathbf{B}\times\mathbf{\Omega})\cdot z] - \sigma^z B_z + \frac{i}{2}\sigma^z\partial_\tau\phi + \frac{v}{2}\partial_x\phi \\ &\quad - \xi(\cos 2\phi - 1)\sigma^x + ievA_0, \end{aligned} \tag{4.22}$$

which represents the interaction of electrons with the order parameter angle ϕ and with the external field $\mathbf{B}$. We consider the case where the magnitude of the interaction is much smaller than the energy gap of the unperturbed system: $|V| \ll \Delta_0$. Specifically, the small parameters in Eq. (4.22) are $\mathbf{B}$, ξ, $\partial_x\phi$ and $\partial_t\phi$. Thus, a perturbative treatment on V does allow to explore arbitrary values of ϕ; such is the gain from the chiral gauge transformation in Sec. 4.1. To second order in V, we have

$$\ln(G_0^{-1} - V) = \ln G_0^{-1} + \ln(1 - G_0V) \approx \ln G_0^{-1} - G_0V - \frac{1}{2}G_0VG_0V. \tag{4.23}$$

Therefore, the perturbative contribution to the order parameter effective action (not including the anomaly part) is

$$S[\phi] = \mathrm{Tr}(G_0V) + \frac{1}{2}\mathrm{Tr}(G_0VG_0V) + S_{\mathrm{ph}}[\phi], \tag{4.24}$$

where we have omitted a term that is independent of ϕ and thus does not contribute to the equation of motion of the order parameter.

4.4.1 First order expansion of the action

Here we focus on the first order contribution of the action, which corresponds to

$$\begin{aligned} \mathrm{Tr}[G_0V] &= \frac{1}{\beta Na}\,\mathrm{tr}\sum_k \langle k|G_0V|k\rangle \\ &= \frac{1}{\beta Na}\,\mathrm{tr}\sum_k \int dx\,d\tau\,\langle k|G_0V|x\rangle\langle x|k\rangle \\ &= \frac{1}{\beta Na}\,\mathrm{tr}\Big[\sum_k G_0(k)\int dx\,d\tau\, -B_x(x)\cos\phi(x)\sigma^x + B_x\sin\phi\,\sigma^y - B_y\cos\phi\,\sigma^y \\ &\quad - B_y\sin\phi\,\sigma^x - \xi(\cos 2\phi - 1)\sigma^x + \frac{i}{2}\sigma^z\partial_\tau\phi + \frac{v}{2}\partial_x\phi - \sigma^z B_z + ievA_0\Big], \end{aligned} \tag{4.25}$$

where tr[...] represents the trace over pseudo-spin indices. Since

$$G_0 = \frac{(i\omega_n - \mu + vk_1\sigma^z + \Delta_0\sigma^x)}{(i\omega_n + \mu)^2 - v^2k_1^2 - \Delta_0^2}, \tag{4.26}$$

we get

$$\mathrm{tr}[B_xG_0\cos\phi\,\sigma^x] = -2B_x\cos\phi\,\frac{\Delta_0}{(i\omega_n + \mu)^2 - v^2k_1^2 - \Delta_0^2}, \tag{4.27}$$

and

$$\mathrm{tr}[G_0\sigma^y] = 0 \tag{4.28}$$

$$\sum_{k_1} \mathrm{tr}[G_0\sigma^z] = 0. \tag{4.29}$$

Since a total derivative term in the Lagrangian has no effect in the equation of motion, it follows that the terms involving $\partial_x\phi$ and $\partial_t\phi$ make no contribution to the effective action at first order. For the rest, we use the same calculational method as in Sec. 3.4 and we arrive at

$$\mathrm{Tr}(G_0V) = \int dx d\tau \left(-\frac{\Delta_0}{a}B_x\tilde{K}_H\cos\phi - \frac{\Delta_0}{a}B_y\tilde{K}_H\sin\phi - \frac{\Delta_0}{a}\tilde{K}_H\xi(\cos 2\phi - 1)\right), \tag{4.30}$$

where we have taken the zero temperature limit. Since we are missing a "kinetic" term from the 1st order expansion(i.e., terms involving $\partial_\tau\phi$ or $\partial_x\phi$), we need to consider the second order contribution.

4.4.2 Second order contribution to the action

Here we compute the second order contribution to the effective action of the order parameter. According to Appendix B,

$$\begin{aligned}\mathrm{Tr}[\frac{1}{2}G_0VG_0V] = &\int dx d\tau \frac{1}{8\pi v}(\partial_\tau\phi)^2 + \frac{i}{2\pi}e\phi(x)\partial_0A_1 \\ &-\left[\frac{1}{8\pi v} - \frac{1}{2v}\mathrm{arctanh}\left(\frac{2\mathrm{v}^2}{2\mathrm{v}^2+\Delta_0^2}\right)\right]e^2v^2A_1^2,\end{aligned} \tag{4.31}$$

where we have only kept the leading order derivatives terms. At first glance, the result is problematic. It is neither Lorentz invariant nor gauge invariant. The problem of gauge non-invariance is the most serious one. This is because Eq. (4.65) is obtained by doing the Matsubara sum first, followed by the momentum sum. If we reverse the order between Matsubara sum and the momentum sum, we still get the same result if the momentum sum has a finite cutoff. To keep the lorentz invariance, one needs to do the momentum sum first from $-\infty$ to ∞, then do the Matsubara sum. So according to Appendix C the result is

$$\begin{aligned}\mathrm{Tr}[\frac{1}{2}G_0VG_0V] = &\int d\tau dx\ \frac{1}{8\pi v}(\partial_\tau\phi)^2 + \frac{1}{8\pi}v(\partial_x\phi)^2 + \frac{i}{2\pi}e\phi(x)\partial_0A_1 - \frac{i}{2\pi}ve\phi\,\partial_1A_0 \\ &-\left[\frac{1}{8\pi v} - \frac{1}{2v}\mathrm{arctanh}\left(\frac{2\mathrm{v}^2}{2\mathrm{v}^2+\Delta_0^2}\right)\right]e^2v^2A_1^2 + \frac{1}{8\pi}ve^2A_0^2.\end{aligned} \tag{4.32}$$

4.4.3 The effective action

There is also a phonon-only action $S_{\rm ph}$ which should be included in the total effective action. This action has been presented above in Eq. (3.15). Here, we will rewrite it using the coordinates (Δ,ϕ). To that end, the following relations are useful:

$$\begin{aligned}\partial_\tau \Delta_x(x,\tau) &= \partial_\tau \frac{\Delta_0 \sin\phi}{2\alpha_S} = \frac{\Delta_0}{2\alpha_s}\partial_\tau\phi\cos\phi,\\ \partial_\tau \Delta_z(x,\tau) &= -\partial_\tau \frac{\Delta_0}{\alpha_H}\cos\phi = \frac{\Delta_0}{\alpha_H}\partial_\tau\phi\sin\phi,\end{aligned} \tag{4.33}$$

Then, the phonon-only action is

$$\begin{aligned}S_{\rm ph}[\phi] &= \int d\tau dx \frac{1}{2a}\Delta_0^2\cos^2\phi\left[\frac{\tilde K_S}{\omega_S^2}(\partial_t\phi)^2-\tilde K_H\right]+\frac{1}{2a}\Delta_0^2\sin^2\phi\left[\frac{\tilde K_H}{\omega_H^2}(\partial_t\phi)^2-\tilde K_S\right]\\ &= \left(\gamma-\frac{2}{a}\Delta_0\xi\right)\int d\tau dx\sin^2\phi+\int d\tau dx\frac{1}{2a}\Delta_0^2\cos^2\phi\frac{\tilde K_S}{\omega_S^2}(\partial_t\phi)^2\\ &+\int d\tau dx\frac{1}{2a}\Delta_0^2\sin^2\phi\frac{\tilde K_H}{\omega_H^2}(\partial_t\phi)^2.\end{aligned} \tag{4.34}$$

Combining with Eq. (4.17), Eq. (4.30) and Eq. (4.32) we get the total effective action in real time is

$$\begin{aligned}S_{\rm eff}[\phi] = \int dxdt\Big(&\frac{1}{4\pi v}(\partial_t\phi)^2-\frac{1}{4\pi}v(\partial_x\phi)^2-\frac{\gamma}{2}(\cos 2\phi-1)-\frac{1}{\pi}e\phi E_x\\ &+\frac{1}{2a}\Delta_0^2(\partial_t\phi)^2\left[\frac{\tilde K_S}{\omega_S^2}\cos^2\phi+\frac{\tilde K_H}{\omega_H^2}\sin^2\phi\right]-\frac{\Delta_0}{a}\tilde K_H B_x\cos\phi-\frac{\Delta_0}{a}\tilde K_H B_y\sin\phi\Big).\end{aligned} \tag{4.35}$$

4.5 Problems

Our derivation of the Eq. (4.35) hides three important problems, which we now list.

4.5.1 Problem of non-gauge invariance

Our expression for $\mathrm{Tr}[G_0VG_0V]$ is not gauge invariant. This is obvious in Eq. (4.65). By revising the order between Matsubara sum and momentum sum, we obtained Eq. (4.32), which does not seem gauge invariant. Notwithstanding the fact that a non-commutativity between Matsubara and momentum sum is a sign of alert, even Eq. (4.32) has a problem. In it, we omitted terms that are second order in A_0 and A_1. If we keep those terms, our result for $\mathrm{Tr}[G_0VG_0V]$ breaks gauge invariance no matter the ordering between Matsubara sum and momentum sum.

4.5.2 Problem of non-commutation of ω_n and k_1

As mentioned in the previsous section, $\sum_{\omega_n}$ and $\int dk_1$ does not commute in the sense that if we do the sum over frequencies first we get Eq. (4.65). However if we do the integral first we get Eq. (4.32). Why don't the two operations commute?

4.5.3 Problem of "fractional charge"

It is well-known from SSH literature that domain walls between $\phi = \pi/2$ and $\phi = -\pi/2$ host a fractional charge of $e/2$ [15]. However in Eq. (4.35) we have $\frac{1}{\pi}e\phi E_x$ instead of $\frac{1}{2\pi}e\phi E_x$. This is because the Jacobian gives a $\frac{1}{2\pi}e\phi E_x$ and $\mathrm{Tr}[\frac{1}{2}G_0VG_0V]$ gives another $\frac{1}{2\pi}e\phi E_x$. Combining the two gives an integer charge for the edge mode, which is certainly incorrect. Why is this so?

4.6 Solution to the problems

All of the problems listed in Sec. 4.5 oringinate from the fact that $\mathrm{Tr}[G_0VG_0V]$ involves a singularity integral. The integral in question is (see Appendix C)

$$\int_0^\infty dk_0 dk_1 \frac{(-k_0^2+v^2k_1^2+\Delta_0^2)}{(k_0^2+v^2k_1^2+\Delta_0^2)^2} = \int_0^{2\pi} d\theta \int_0^\infty dr \frac{1}{v} r \frac{\Delta_0^2 - r^2\cos 2\theta}{(r^2+\Delta_0^2)^2}. \tag{4.36}$$

This integral is ill-defined, in the sense that

$$\int_0^\infty dr \frac{r^3}{(r^2+\Delta_0^2)^2} \to \infty, \tag{4.37}$$

and

$$\int_0^\infty d\theta \cos 2\theta = 0. \tag{4.38}$$

Thus, we have a case of $0\times\infty$, which is ill-defined. This kind of problematic integral is well-known in quantum field theory. One recipe to solve the problem is to regularize $\mathrm{Tr}[G_0VG_0V]$ following the Pauli-Villars regularization [26]. This consists of replacing

$$\frac{(-k_0^2+v^2k_1^2+\Delta_0^2)}{(k_0^2+v^2k_1^2+\Delta_0^2)^2} \to \frac{(-k_0^2+v^2k_1^2+\Delta_0^2)}{(k_0^2+v^2k_1^2+\Delta_0^2)^2} - \frac{(-k_0^2+v^2k_1^2+M^2)}{(k_0^2+v^2k_1^2+M^2)^2}, \tag{4.39}$$

where M is a large-momentum cutoff that is taken to ∞ at the end. Then Eq. (4.36) becomes

$$\int_0^\pi d\theta \int_0^\infty dr\ \frac{1}{v} r \left[\frac{\Delta_0^2}{(r^2+\Delta_0^2)^2} - \frac{M^2}{(r^2+M^2)^2}\right] = 0. \tag{4.40}$$

This is a remarkable result. It means that Eq. (4.65) and Eq. (4.32) should be replaced with zero. This does not mean that the regularized $\mathrm{Tr}[G_0VG_0V]$ is exactly zero: it has

higher order derivative terms in ϕ and in the gauge fields, but those terms are small compared to the ones that appear in the chiral anomaly action. They can therefore be neglected. Another bonus of the Pauli-Villars regularization is that the A_0^2 and A_1^2 that broke gauge invariance will be canceled. Finally, once we regularize $\mathrm{Tr}[G_0 V G_0 V]$, the result is independent of the ordering between the Matsubara sum and momentum sum.

4.7 Comparing with previous works

In the course of our work, we noticed a number of related previous works that investigated the dynamics of incommensurate charge density waves (ICDW) [9, 41, 34, 24, 18]. By ICDW, it is meant that the energy of the system is independent of ϕ. In all these papers, the calculation of $\mathrm{Tr}[G_0 V G_0 V]$ and the role of the chiral anomaly are discussed in some form.

In [9] the authors claim that all the contributions to the action come from the regular $\mathrm{Tr}[G_0 V G_0 V]$ term and they do not consider the Jacobian term. We think their argument is not fully correct because $\mathrm{Tr}[G_0 V G_0 V]$ has singular part and needs to be regularized. Also, their expression for $\mathrm{Tr}[G_0 V G_0 V]$ is not gauge-invariant either.

In [41] the authors use a very different regularization, that is not Lorentz invariant or gauge invariant, and they choose a finite momentum cut-off which does not preserve Lorentz invariance. Actually, their treatment is half relativistic and half non-relativistic. The authors claim that part of the regular term $\mathrm{Tr}[G_0 V G_0 V]$ and part of the Jacobian term contribute to the action, and the combined term is gauge invariant. The authors get the standard answer, however their method is non-standard because normally the regularization should be gauge invariant.

In [24] the authors claim that $\mathrm{Tr}[G_0 V G_0 V]$ does not contribute to the action at leading order and that all the leading contributions come from the anomaly term. Their conclusion matches our result. However, they claim that $\mathrm{Tr}[G_0 V G_0 V]$ can be neglected is not substantiated by an explicit calculation. As we have seen, an explicit calculation shows that $\mathrm{Tr}[G_0 V G_0 V]$ is of the same order as the anomaly term if one forgets to regularize it.

In [34, 18] the authors use different approaches from ours. The effective action is computed by different methods and they use a different regularization. Our result matches their result.

Comparing with all these papers, the main novelties in our result is that (i) we consider a commensurate charge density wave with non-zero anisotropy energy; (ii) we consider the effect of external perturbations beyond a simple electric field (i.e. we consider B_x and B_y); (iii) we week to realize a proof of principle for a topological bit. The points (i) and (ii) are essential for the point (iii); as such, our work is distinct from the earlier literature on the dynamics of charge density waves.

We also notice that some well-cited papers, such as [40], claim that there is no chiral anomaly for massive fermions because the axial current is conserved in that case. By axial current, it is meant the difference in the currents of the left-moving fermions

and right-moving fermions. However, there is no contradiction with our result, because by "anomaly contribution" we mean the Jacobian contribution and the axial current is indeed conserved. However, even the axial current is conserved the Jacobian term can still lead to observable effect. The axial current conservation is

$$\langle \partial_\mu j_5^\mu \rangle = 2\langle M\bar{\Psi}\sigma^z\Psi\rangle + \frac{e}{2\pi}\epsilon_{\mu\nu}\langle \tilde{F}_{\mu\nu}\rangle, \tag{4.41}$$

where j_5 is the axial current and M is the fermion mass. When the fermion mass is non-zero, then the axial current should be conserved such that $\langle \partial_\mu j_5^\mu \rangle = 0$, this is because due to the presence of the mass gap, there is no net left mover nor right mover been created by the external electric field. Such argument agrees with the semiclassical electron dynamics in band theory [4]. Consequently, the Jacobian terms would still contribute to the action (second term on the right-hand side of Eq. (4.41)) because it needs to be there to cancel the mass contribution. We noticed a similar result has been obtained in [37] independently.

4.8 Equation of motion of the phonon order parameter

In this section we derive the equation of motion for the phonon order parameter, which is a topological analogue of the Landau-Lifshitz-Gilbert equation for the magnetization in a ferromagnet. The effective action is

$$S_{\text{eff}}[\phi] = \text{Tr}[G_0 V] + S_a[\phi] + S_{\text{ph}}[\phi]. \tag{4.42}$$

Assuming for simplicity$\omega_S^2 = \omega_H^2$, the magnetization of effective action with respect to ϕgives the equation of motion

$$(1+\eta)\partial_t^2\phi - v^2\partial_x^2\phi + 4\pi v\gamma \sin 2\phi + \eta\omega_H^2 B_x \sin\phi - \eta\omega_H^2 B_y \cos\phi + 4\pi e v E_x = 0, \tag{4.43}$$

where η is defined as

$$\eta = \frac{4\pi v \Delta_0^2 \tilde{K}_H}{a\omega_H^2} \tag{4.44}$$

the ground state and the external perturbations are spatially uniform, then the equation of motion reduces to

$$(1+\eta)\partial_t^2\phi + 4\pi v\gamma \sin 2\phi + \eta\omega_H^2 B_x \sin\phi - \eta\omega_H^2 B_y \cos\phi + 4\pi e v E_x = 0. \tag{4.45}$$

The equation of motion describes the motion of a sliding commensurate CDW pinned by phonon anisotropy γ. It is well-known that impurities could pin the CDW [16], and we showed that the phonon anisotropy γ can also pin the CDW.

4.9 Effective action of the phonon order parameter involving damping

In order to form a bit there should be a possibility of transition between two different states. In our model, we know that if ϕ moves from the local minimum $\phi = \frac{\pi}{2}$ to local minimum $\phi = -\frac{\pi}{2}$, then we can reverse the sign of order parameter Δ_x and induce a topological phase transition. However, if there is no energy loss, ϕ will permanently move between the two local minima, which is not good for creating a topological bit. In order to stabilize ϕ at one of the local minima, $\phi = \frac{\pi}{2}$ or $\phi = -\frac{\pi}{2}$, the system needs to dissipate energy, in other words, the system needs to be damped.

Damping of the system mainly comes from two main contributions: electrons and phonons. The mechanism for damping originating from electrons is the creation of electron-hole pairs from residual fluctuations of the order parameter, which eventually annihilate into phonons and thus dissipate energy. However, at zero temperature and when the characteristic frequency of the dynamics of the order parameter is smaller than the energy gap (which we have assumed above int he perturbative analysis), then this process is suppressed.

According to the pioneering works of Leggett and co-authors on the Caldeira-Leggett model and environmental effect on spin-boson systems [7], even a small fluctuation from the environment will cause energy dissipation in the system.

Let us connect the system to a dissipating environment. Dissipation actions $S_{\text{env}}[\Delta_x]$ and $S_{\text{env}}[\Delta_z]$ describe the interactions of the SSH order parameter with the environment and the Holstein order parameter with the environment respectively, then the phonon-only part action becomes

$$S_{\text{ph}}[\Delta_x, \Delta_z] = S_{\text{bulk}}[\Delta_x, \Delta_z] + S_{\text{env}}[\Delta_x] + S_{\text{env}}[\Delta_z], \tag{4.46}$$

with the dissipation action, $\delta S = 0$ describes the equation of motion including damping. The bulk part of the phonon-only action obtained from Chapter 3 is given by

$$S_{\text{bulk}}[\Delta_x, \Delta_z] = \frac{1}{2} m_s \int dx d\tau [(\partial_\tau \Delta_x)^2 + 4\alpha_S^2 \omega_S^2 \Delta_x^2] + \frac{1}{2} m_H [(\partial_\tau \Delta_z)^2 + \alpha_H^2 \omega_H^2 \Delta_z^2]. \tag{4.47}$$

In the Caldeira-Leggett model, the dissipation part of the action is [3]

$$\begin{aligned} S_{\text{env}}[\Delta_x] &= \int dx d\tau dx' d\tau' \ \Delta_x(x,\tau) K_{\Delta_x}(x-x', \tau-\tau') \Delta_x(x',\tau') \\ S_{\text{env}}[\Delta_z] &= \int dx d\tau dx' d\tau' \ \Delta_z(x,\tau) K_{\Delta_z}(x-x', \tau-\tau') \Delta_z(x',\tau') \end{aligned} \tag{4.48}$$

where

$$K_{\Delta_x}(x,\tau) = \int_0^\infty d\omega\, J_{\Delta_x}(\omega) D_\omega(x,\tau)$$
$$K_{\Delta_z}(x,\tau) = \int_0^\infty d\omega\, J_{\Delta_z}(\omega) D_\omega(x,\tau) \tag{4.49}$$

and D_ω is the phonon Green function, in the Fourier space [3]

$$D_\omega(\omega_n) = \frac{\omega_n^2}{\omega(\omega^2+\omega_n^2)}, \tag{4.50}$$

where ω is the frequency of external phonon (phonons from the environment) modes, ω_n is the Matsubara frequency of the SSH and Holstein phonon modes. And

$$J_{\Delta_x}(\omega) = \tilde{\Gamma}_S|\omega|$$
$$J_{\Delta_z}(\omega) = \tilde{\Gamma}_H|\omega| \tag{4.51}$$

are the ohmic interactions for SSH and Holstein order parameters with the environment. Where $\tilde{\Gamma}_S$ represents the coupling between a SSH-type phonon with the environment, and $\tilde{\Gamma}_H$ represents the coupling between a Holstein-type phonon with the environment. The ohmic interactions break the time-reversal symmetry of the system. In real time, we get [3]

$$S_{\text{env}}[\Delta_x,\Delta_z] = \int dx dt dt' \tilde{\Gamma}_S \left(\frac{\Delta_x(t,x)-\Delta_x(t',x)}{t-t'}\right)^2 + \tilde{\Gamma}_H \left(\frac{\Delta_z(t,x)-\Delta_z(t',x)}{t-t'}\right)^2, \tag{4.52}$$

4.9.1 Equation of motion of the phonon with damping term

Using the chain rule,

$$\frac{\delta S_{\text{env}}}{\phi} = \frac{\delta S_{\text{env}}}{\delta\Delta_x}\frac{\delta\Delta_x}{\delta\phi} + \frac{\delta S_{\text{env}}}{\delta\Delta_z}\frac{\delta\Delta_z}{\delta\phi}. \tag{4.53}$$

Also, we write t' to Fourier space [39]

$$\begin{aligned}\frac{\delta S_{\text{env}}}{\delta\Delta_x} &= \int dt'\, \tilde{\Gamma}_S \frac{2\left(\Delta_x(x,t)-\Delta_x(x,t')\right)}{(t-t')^2} = \int dt'\, \tilde{\Gamma}_S \left(\Delta_x(x,t)-\Delta_x(x,t')\right) D(t-t') \\ &= \int d\omega\, \tilde{\Gamma}_S [D(\omega)-D(0)]\Delta_x(\omega,x)e^{-i\omega t} \\ &= \int d\omega\, \tilde{\Gamma}_S \left[i\omega\frac{\text{Im}\, D(\omega)}{\omega} + \omega^2\frac{\text{Re}\,(\text{D}(\omega)-\text{D}(0))}{\omega^2}\right]\Delta_x(\omega,x)e^{-i\omega t},\end{aligned} \tag{4.54}$$

where $-\tilde{\Gamma}_S \,\mathrm{Im}\, D(\omega)/\omega \equiv \Gamma_S$ is the normalized coupling coefficient and $\mathrm{Re}\,(\mathrm{D}(\omega)-\mathrm{D}(0))/\omega^2$ can be absorbed into the mass term. We assume Γ_S is approximately a constant, consequently

$$\frac{\delta S_{\mathrm{env}}}{\delta \Delta_x} = \int dt\ \Gamma_S \partial_t \Delta_x. \tag{4.55}$$

Similarly

$$\frac{\delta S_{\mathrm{env}}}{\delta \Delta_z} = \int dt\ \Gamma_H \partial_t \Delta_z, \tag{4.56}$$

where $-\tilde{\Gamma}_H \,\mathrm{Im}\, D(\omega)/\omega \equiv \Gamma_H$ is the normalized coupling coefficient. So

$$\delta S_{\mathrm{env}} = \int dx dt \left[\Gamma_S \Delta^2 \cos\phi\, \partial_t \sin\phi - \Gamma_H \Delta^2 \sin\phi\, \partial_t \cos\phi\right] \delta\phi \tag{4.57}$$

where we ignore terms involving $\Gamma_S\gamma$ and $\Gamma_H\gamma$. If we set $\omega_S = \omega_H$ and $\Gamma_S = \Gamma_H$, the equation of motion involving damping is

$$(1+\eta)\partial_t^2\phi + 4\pi\gamma \sin 2\phi + \eta\Gamma_H\Delta_0^2\partial_t\phi = -\eta\omega_H^2 B_x \sin\phi + \eta\omega_H^2 B_y \cos\phi - 4\pi e\nu E_x. \tag{4.58}$$

4.10 Analogue with the Josephson effect

In this section, we describe an analogy between Eq. (4.58) and a current-biased Josephson junction. While this analogy has been described in earlier works [16], we identify a novel element that follows from B_x and B_y.

The Josephson effect consists of tunneling of Cooper pairs between two weakly-coupled superconductors [19]. Adopting the Resistively Capacitively Shunted Junction (RCSJ) model, the current conservation equation in a Josephson junction can be approximately described as [25]

$$I_{\mathrm{bias}} = I_0 \sin 2\phi + \frac{1}{eR}\partial_t\phi + \frac{C}{e}\partial_t^2\phi, \tag{4.59}$$

where I_{bias} is the bias current, 2ϕ is the phase difference between the two superconductors, R is the normal-state resistance of the weak link, and C is the junction caacitance. The first term on the right-hand side of Eq. (4.59) describes the dissipationless current due to the tunneling of Cooper pairs, with its maximum amplitude given by I_0. The second term on the right-hand side of Eq. (4.59) describes the normal (quasiparticle) dissipative current, while the third term on the right-hand side describes Maxwell's displacement current.

It is clear that, if we take $B_x = B_y = 0$, Eq. (4.59) has the same form as Eq. (4.58). This analogy was first recognized in Refs. ([9, 16]). Modulo numerical factors, the correspondence between the Josephson junction and the CDW goes as follows: (1)

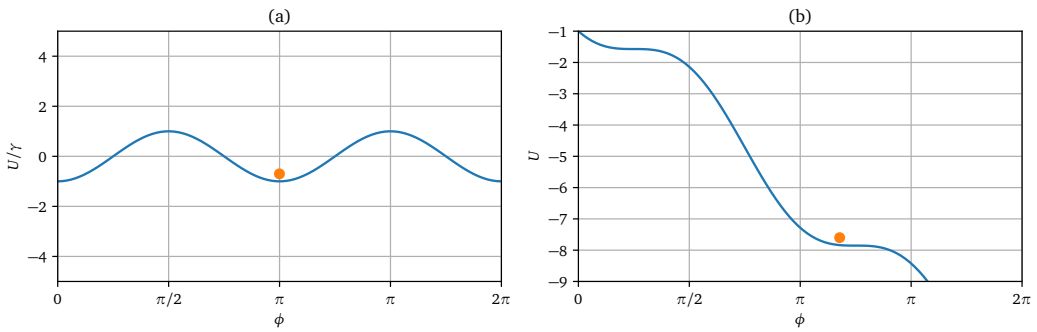

Figure 4.1
Pinning Potential for ϕ. Panel A represents the case where the charge density wave is localized, in the plot $eE_x/\gamma = 0$. Panel B represents the case where the electrical field can move the charge density wave, in the plot $eE_x/\gamma = 2$

$\phi \longleftrightarrow \phi$; (2) $I_0 \longleftrightarrow$ anisotropy energy γ; (3) dissipative current $\longleftrightarrow$ damping term; (4) displacement current $\longleftrightarrow$ inertial term; (5) $I_{\text{bias}} \longleftrightarrow E_x$.

Taking advantage of the analogy with the Josephson effect, we can anticipate the effect of the electric field in the dynamics of the charge density wave. To that end, we first recognize that (still for $B_x = B_y = 0$) Eq. (4.58) can be understood as the equation of motion of an effective particle moving in a titled washboard potential.

$$U[\phi] = 2\pi\gamma \cos 2\phi - eE_x\phi, \tag{4.60}$$

where ϕ plays the role of the position of the particle. If $|eE_x| < 4\pi\gamma$, then there will be a steady-state solution and ϕ is a constant. In this case, E_x along cannot induce a topological phase transition. Graphically, this situation is represented in Fig. (4.1).

For $|E_x| > 4\pi\gamma/e$, the effective particle keeps sliding down the washboard potential. This situation is represented graphically in Fig. (4.1B). In this case, while the electric field is on, the system undergoes a succession of topological phase transitions. Once the electric field is turned off, the system will once again relax towards a local minimum of the untilted washboard potential, aided by the damping. If the final and the initial values of ϕ differ by ϕ (modulo 2π), then we will have realized a permanent topological phase transition with a transient electric field. We will discuss this transition further below.

Thus far, we have considered $B_x = B_y = 0$. In earlier works of the dynamics of charge density waves, B_x and B_y are not included. Yet, there is interesting physical content associated with them. For example, when $B_x \neq 0$, we get a new supercurrent-like term with a doubled periodicity in ϕ: in Eq. (4.58), B_x multiplies $\sin\phi$ while γ multiplies $\sin 2\phi$. Therefore, a constant $B_x \neq 0$ gives rise to an effect that is analogous to the fractional Josephson effect. Recently, the fractional Josephson effect has attracted a lot of interest in Josephson junctions made out of topological superconductors [1]. In these systems, Majorana bound states are responsible for the fractional Josephson effect. Intense efforts have been devoted to detect such an effect through unconventional

Shapiro steps and Josephson radiation, for example. It is potentially interesting and new that an analogue of the fractional Josephson effect could also take place in charge density wave systems. In addition, the effect of B_y is also unconventional in the sense that it multiplies a $\cos\phi$ factor in Eq. (4.58). The analogy of this term in Josephson junctions needs to be further investigated.

4.11 Permanent topological phase transition from transient perturbations

In this section, we respond affirmatively to the central question of this thesis: can a transient external perturbation (E_x, B_x, B_y) induce a permanent topological phase transition? By doing so, we provide a proof of concept for the topological analogue of the magnetic bit.

As usual, we place ourselves in the regime with $\gamma<0$. Then, without external perturbations, the system will be in either one of the degenerate ground states which corresponds to $\phi = \frac{\pi}{2} (\mathrm{mod} 2\pi)$ and $\phi = \frac{3\pi}{2} (\mathrm{mod} 2\pi)$ respectively. The two ground states are topologically distinct, which means that for a finite chain there is a localized zero-energy electronic edge mode in one ground state, and no such mode in the other.

With an external perturbation (E_x, B_x, B_y) turned on, we are interested in what pulse shape of the perturbations can induce the topologically non-trivial phase transition. Then we will be able to construct a topological bit as an analogue of a magnetic bit.

To that end, we will solve Eq. (4.58) numerically. Let us rewrite that equation in a dimensionless form that is suitable for computer calculation. We define the characteristic time of the anisotropy field as

$$\frac{1}{\tau_a^2} = -4\pi\nu\gamma, \tag{4.61}$$

and the characteristic times of the external fields to be

$$\begin{aligned}
\frac{1}{\tau_{B_x}^2} &= 8\pi t_0 \tilde{K_H} \Delta_0^2 B_x, \\
\frac{1}{\tau_{E_x}^2} &= 4\pi\nu e E_x, \\
\frac{1}{\tau_{B_y}^2} &= 8\pi t_0 \tilde{K_H} \Delta_0^2 B_y,
\end{aligned} \tag{4.62}$$

and the characteristic damping time to be

$$\frac{1}{\tau_d} = \eta\Gamma. \tag{4.63}$$

Moreover we will use a dimensionless time

$$\bar{t} = \frac{t}{\tau_a}, \tag{4.64}$$

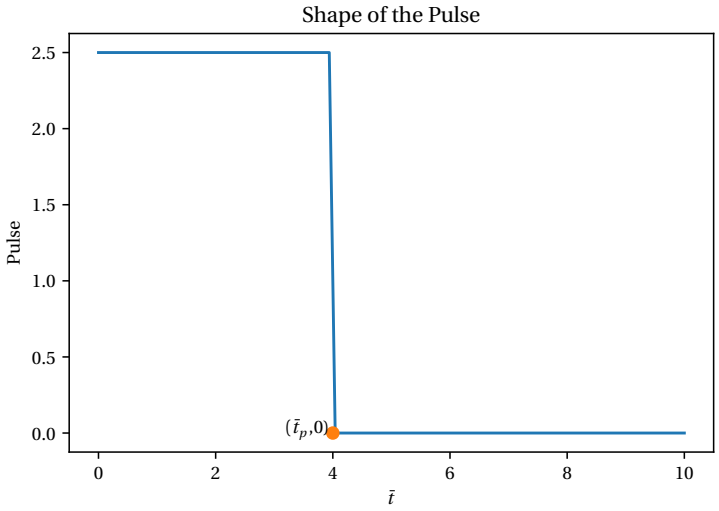

Figure 4.2
An example of the shape of the pulse. The value of the pulse is $(\overline{B_x}\cos\phi + \overline{E_x})\Theta(\bar{t}_p - \bar{t})$, where we take $\overline{B_x} = 0$, $\overline{E_X} = 2.5$, $\bar{t}_p = 4$, and Θ is the Heaviside function.

which amounts to setting $1/\tau_a$ as the unit of time. Proceeding to the appropriate changes in Eq. (4.58), we find

$$(1+\eta)\partial_{\bar{t}}^2\phi - \sin 2\phi + \overline{B_x}\sin\phi - \overline{B_y}\cos\phi + \overline{E_x} + \Gamma\partial_{\bar{t}}\phi = 0, \tag{4.65}$$

where we have defined the dimensionless coefficients $\overline{B_x} = \tau_a^2/\tau_{B_x}^2$, $\overline{B_y} = \tau_a^2/\tau_{B_y}^2$, $\overline{E_x} = \tau_a^2/\tau_{E_x}^2$ and $\Gamma = \tau_a/\tau_d$.

For correctness, we take the initial state of the system (before the perturbation is switched on) to be $\phi = \pi/2$. Solving Eq. (4.65) for transient perturbations, we will obtain the final state at long times (well after the perturbation is switched off). If the final state turns out to be $\phi = \frac{\pi}{2} + (2n+1)\pi$ for n in $\mathbb{Z}$, we will have achieved the desired topological phase transition.

The numerical results for the aforementioned final state are displaced in Figs. (4.3), (4.4) and (4.5), for different damping strengths. The red color corresponds to a final state that is topologically different from the initial state ($\phi = \frac{\pi}{2} + (2n+1)\pi$). The blue color corresponds to a final state that is topologically equivalent to the initial state ($\phi = \frac{\pi}{2} + 2n\pi$). In these figures, we take $B_y = 0$ but we allow for non-zero E_x and B_x. For the latter, we consider pulses with finite duration $\bar{t}_p$, a graph for a pulse is given in Fig .(4.2).

We can see in all the solution diagrams there exists a critical value of E_x beyond which the topological phase transition is realized. This critical value of E_x does not depend on the damping strength. This is consistent with the analytical discussion about the tilted washboard potential in Sec. 4.10. The diagrams contain many "arcs" (for

example in the left lower corner of Fig. 4.3), which are caused by the inertia of CDW. Even when the pulse stops, the CDW will continue to move until it is finally stopped by damping.

For larger values of B_x, the red regions in the figures become overall wider. In other words, B_x helps realize the desired topological phase transition. To understand why that is the case, we recall that B_x multiplies $\sin\phi$ in the equation of motion, while the anisotropy field scales as $\sin 2\phi$. Thus, in the effective potential energy, B_x will be accompanied by $\cos\phi$, while the anisotropy energy will scale as $\cos 2\phi$. Because $\cos\phi$ is different for $\phi = \pi/2$ and $\phi = -\pi/2$. Plotting combined $\cos 2\phi$ and $\cos\phi$ functions, we see that B_x reduces the energy barrier for transitions between topologically distinct states (e.g. $\phi \to \phi + \pi$), while it increases the energy barrier for transitions between topologically identical transitions (e.g $\phi \to \phi + 2\pi$).

When the duration of the pulse t_p increases, the patterns of the final state diagrams repeat themselves. This is because the effective potential of the CDW is approximately periodic in ϕ. Admittedly, due to the ϕE_x term in the potential, the value of the potential itself is not periodic, however, the value of ϕ which minimizes the potential energy is periodic since the derivative of the potential is periodic.

In all the graphs there exists a critical value of t_p beyond which the topological phase transition is realized. An easy thought experiment is assuming t_p to be a Dirac-delta function $t_p = \delta(0)$, then weather how strong the external perturbations are, they will not contribute to the equation of motion (Eq. (4.65)). Both B_x and E_x have significant impacts on the critical value of t_p.

When E_x is large, a small increase of t_p/τ_a leads to a large change of ϕ in the final state. This is why successive blue and red arcs get closer at stronger electric fields. As a result, for strong E_x, it is harder to predict whether final value of ϕ will end being the "correct" one (red) or the "wrong" one (blue). An easy thought experiment is assuming the E_x becomes infinite, in that case, the final value of ϕ becomes unpredictable.

When damping becomes weaker, the final state diagrams become more chaotic, and it is harder to predict whether final value of ϕ will end being the "correct" one (red) or the "wrong" one (blue). This is because, with weaker damping, the system behaves closer to the undamped case, for which the "particle" moves constantly and never localizes.

In conclusion, the optimal set of parameters that helps to realize the topological bit are: (i) strong damping; (ii) E_x exceeding critical value; (iii) non-zero B_x; (iv) t_p exceeding critical value.

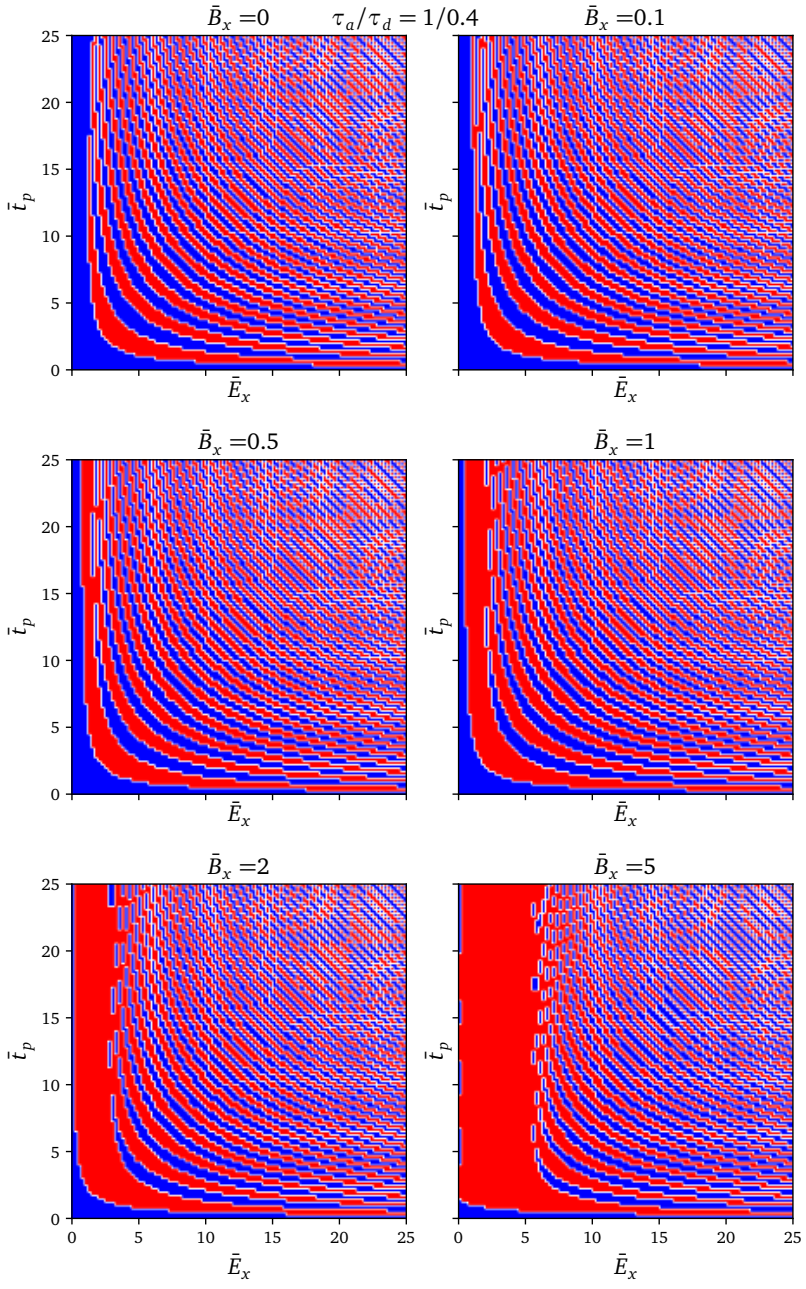

Figure 4.3
Phase diagram for strong damping. Blue: initial topology; Red: Different topology. E_x is the dimensionless electrical field, B_x is the dimensionless pseudo magnetic field in x direction. t_0/τ_a is the characteristic time for the lifetime of the plus, where we take the equation of motion to be: $\partial_{\bar{t}}^2\phi - \sin 2\phi + (B_x \sin\phi + E_x)\,\Theta(\bar{t}_p - \bar{t}) + \frac{1}{0.4}\partial_{\bar{t}}\phi = 0$, Θ is the Heaviside step function.

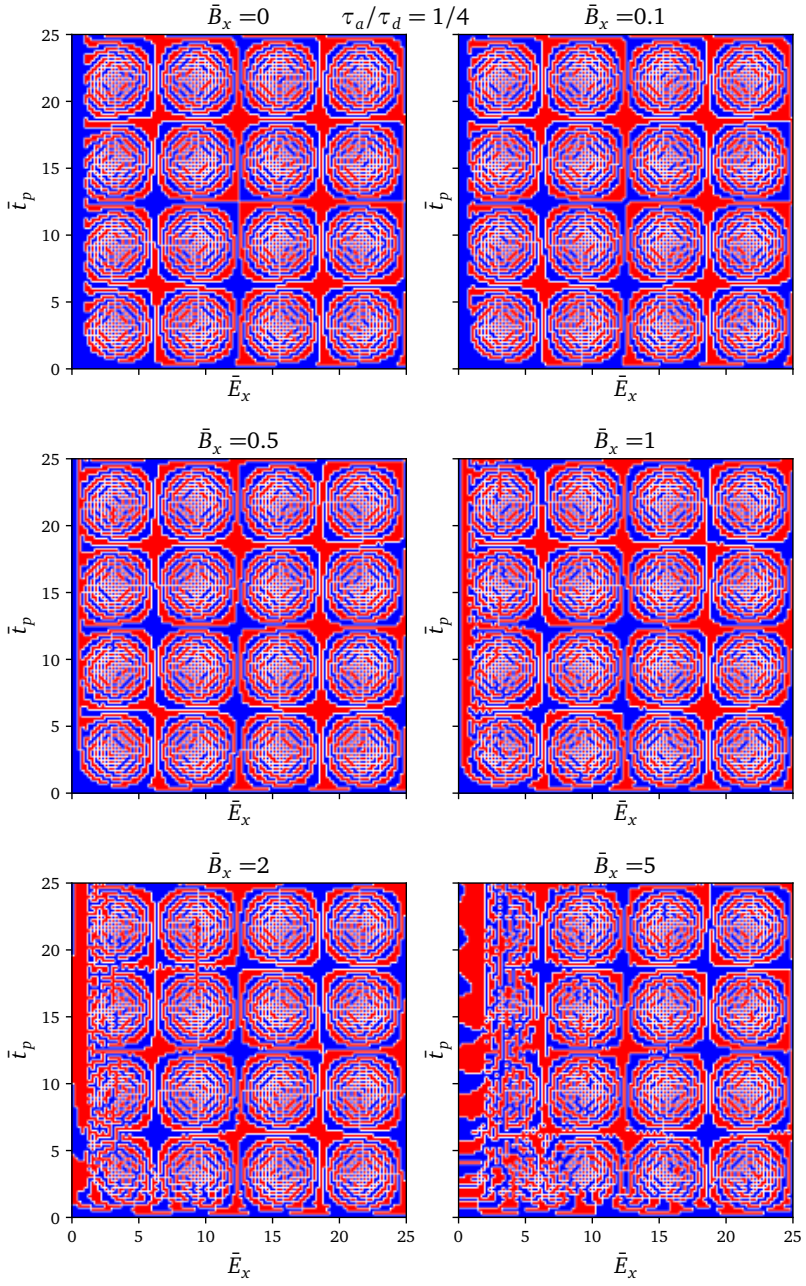

Figure 4.4
Phase diagram for medium damping. Blue: initial topology; Red: Different topology. E_x is the dimensionless electrical field, B_x is the dimensionless pseudo magnetic field in x direction. t_0/τ_a is the characteristic time for the lifetime of the plus, where we take the equation of motion to be: $\partial_{\bar{t}}^2\phi - \sin 2\phi + (B_x \sin\phi + E_x)\,\Theta(\bar{t}_p - \bar{t}) + \frac{1}{4}\partial_{\bar{t}}\phi = 0$, Θ is the Heaviside step function.

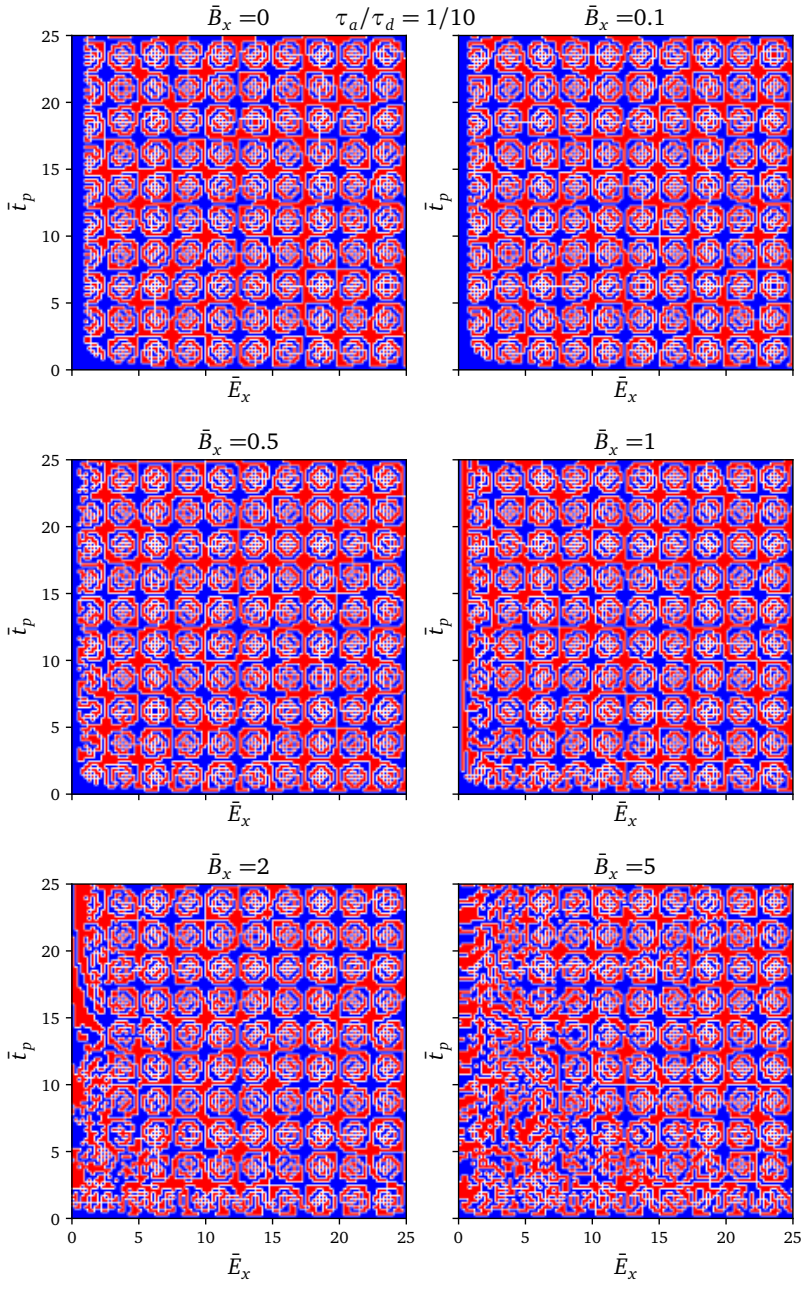

Figure 4.5
Phase diagram for weak damping. Blue: initial topology; Red: Different topology. E_x is the dimensionless electrical field, B_x is the dimensionless pseudo magnetic field in x direction. t_0/τ_a is the characteristic assuming the lifetime of the plus, where we take the equation of motion to be: $\partial_{\bar{t}}^2\phi - \sin 2\phi + (B_x \sin\phi + E_x)\,\Theta(\bar{t}_p - \bar{t}) + \frac{1}{10}\partial_{\bar{t}}\phi = 0$, Θ is the Heaviside step function.

Chapter 5

Conclusion

In this thesis, I studied the topological phase transition induced by perturbations beyond the general "Floquet" picture. In Floquet engineering, the time-periodic Hamiltonian could change the topological phase of the system, however, the topological phase returns to its initial value when the perturbation is turned off. Is it possible to conceive a system in which a transient external perturbation can lead to a permanent change in the electronic band topology? If such a perturbation exists, then the two phases could form a "topological bit", an analog of the magnetic bit.

In a magnetic memory, a pair of mean-field magnetizations with opposite orientations forms a "magnetic bit". It is well-known that the magnetization could be reversed by external perturbations and remains in the final position. Such dynamics is described by the Landau-Lifshitz-Gilbert equation.

Inspired by the magnetic memory, we constructed and focused on the "SSH-Holstein" model and tried to derive an equation for the topological phase of the system as an analog of the Landau-Lifshitz-Gilbert equation, which could describe the dynamics of the topological phase, and allow the system to remain in its final topological phase even if the perturbation is turned off.

The final-state diagrams are Figs. (4.3), (4.4) and (4.5). The optimal set of parameters that helps to realize the topological bit are: (i) strong damping; (ii) E_x exceeding critical value; (iii) non-zero B_x; (iv) t_0 exceeding critical value.

There are several future directions: (i) As pointed out in Sec. 4.10, it is possible that fractional Josephson effect may take place in charge density wave systems without the appearance of Majorana fermions; (ii) physical meaning of anomaly term $E_x\phi$. We attempt to link ϕ to the polarization; (iii) is it possible to generalize our method in this thesis to different systems? More works need to be done.

Appendix A

Detailed calculations of the chiral anomaly term in the action

In Chapter 4, we attempt to calculate the anomaly contribution to the effective action, in this appendix, we are performing the detailed calculations. Recall the chiral gauge transformation we used in the previous section is

$$\Psi = \exp\left(-i\frac{\sigma_z\phi}{2}\right)\Psi', \tag{A.1}$$

and since $[\sigma_x, \sigma_z]_+ = 0$ we get

$$\bar{\Psi} = \bar{\Psi}' \exp\left(-i\frac{\sigma_z\phi}{2}\right), \tag{A.2}$$

after the gauge transformation the action stays the same. However, the measure should change to $D[\Psi, \bar{\Psi}] \to D[\Psi', \bar{\Psi}']\det(J)^{-2}$ since $\bar{\Psi}, \Psi$ are fermionic fields. We expand the fields $\Psi, \bar{\Psi}$ in the basis of eigenfunctions of iD:

$$\begin{aligned} \Psi &= \sum_k a_n \psi_n(x) \\ \bar{\Psi} &= \sum_n b_n \psi_n(x), \end{aligned} \tag{A.3}$$

where a_n, b_n are Grassmann numbers [13]. After the gauge transformation

$$\begin{aligned} \Psi' &= \sum_n a'_n \psi_n(x) \\ \bar{\Psi}' &= \sum_n b'_n \psi_n(x), \end{aligned} \tag{A.4}$$

so

$$a'_n = \langle\psi_n|\Psi'\rangle = \langle\psi_n|\exp\left(-i\frac{\sigma_z\phi}{2}\right)|\Psi\rangle$$
$$= \sum_m \langle\psi_n|\exp\left(-i\frac{\sigma_z\phi}{2}\right)|\psi_m\rangle\langle\psi_m|\Psi\rangle = \sum_m J_{mn}a_m, \tag{A.5}$$

where the Jacobian J is

$$J_{mn} = \frac{\delta a'_n}{\delta a_m} = \langle\psi_n|\exp\left(-i\frac{\sigma_z\phi}{2}\right)|\psi_m\rangle. \tag{A.6}$$

First we assume ϕ to be infinitesimal ($\phi \to \delta\phi$). Then the Jacobian is given by

$$\det(J)^{-2} = \exp[-2\ln \mathrm{Tr} J]$$
$$= \exp\Big[-2\ln\sum_n \mathrm{tr}\int d\tau dx \psi_n^\dagger(\tau,x)\exp\left(-i\frac{\sigma_z\delta\phi}{2}\right)\psi_n(\tau,x)\Big]$$
$$\approx \exp\Big[-2\ln\sum_n \mathrm{tr}\int d\tau dx \psi_n^\dagger(\tau,x)(1-i\frac{\sigma_z\delta\phi}{2})\psi_n(\tau,x)\Big] \tag{A.7}$$
$$\approx \exp\Big[2i\sum_n \mathrm{tr}\int d\tau dx \psi_n^\dagger\frac{\sigma_z\delta\phi}{2}\psi_n\Big]. \tag{A.8}$$

However, $\sum_n \int dx d\tau \psi_n^+(\tau,x)\psi_n(\tau,x) = \int d\tau dx \delta(0)$ is singular, thus $\det(J)^{-2}$ is ill-defined. We need to regularize this expression, which we do by adding a gauge invariant factor $-\not{D}^2/C^2$ where C^2 is a large momentum scale [38], so the partition function becomes

$$\int D[\Psi,\bar\Psi,\phi]e^{-S'[\Psi,\bar\Psi,\phi]} = \int D[\bar\Psi,\Psi,\phi]\det(J)^{-2}e^{-S[\Psi,\bar\Psi,\phi]}$$
$$= \int D[\bar\Psi,\Psi,\phi]\mathrm{lim}_{C\to\infty}\exp\left[2i\,\mathrm{tr}\int d\tau dx\frac{\delta\phi}{2}\left(\psi_n^\dagger\sigma^z e^{-\not{D}^2/C^2}\psi_n\right)\right]e^{-S[\Psi,\bar\Psi,\phi]}$$
$$= \int D[\bar\Psi,\Psi,\phi]e^{-S_a}e^{S}, \tag{A.9}$$

the regular part action

$$S[\Psi,\bar\Psi,\phi] = \int d\tau dx \bar\Psi\bar G^{-1}\Psi = \int d\tau dx \Psi^+ G^{-1}\Psi \tag{A.10}$$

and the anomaly part action

$$S_a[\Psi,\bar\Psi,\phi] = -2\,\mathrm{Tr}\left(\psi_n^+\phi\sigma^z e^{-\not{D}^2/C^2}\psi_n\right) \tag{A.11}$$

depends on both electrons degree of freedom (Ψ) and the phonon order parameter Δ_{min}. In order to study the dynamics of the phonon order parameter, we would like to know how the electron degrees of freedom affect the phonon order parameter. Transfer to Fourier space we get

$$\begin{aligned}
\exp\left[2i\,\mathrm{Tr}\left(\psi_n^\dagger \frac{\phi}{2}\sigma^z e^{-\not{D}^2/C^2}\psi_n\right)\right] &= \exp\left[\frac{i}{4\pi^2}\int d\tau dx\,\mathrm{tr}\int dk\sigma^z e^{\frac{-k^2}{C^2}+\frac{1}{4C^2}[\gamma^\mu,\gamma^\nu]\tilde{F}_{\mu\nu}}\phi\right] \\
&\approx \exp\left[\frac{i}{16\pi^2C^2}\int d\tau dx\,\mathrm{tr}\int dk\sigma^z[\gamma^\mu,\gamma^\nu]\tilde{F}_{\mu\nu}\phi e^{-k^2/C^2}\right] \\
&= \exp\left[\int d\tau dx\frac{-i}{4\pi}\epsilon^{\mu\nu}\tilde{F}_{\mu\nu}\phi\right] \\
&= \exp\left[\frac{-i}{2\pi}\int d\tau dx\; e\phi E_x - \frac{1}{4\pi\nu}(\partial_\tau\phi)^2 - \frac{\nu}{4\pi}(\partial_x\phi)^2\right], \qquad \text{(A.12)}
\end{aligned}$$

where $k=(k_0,k_1)$ and $\tilde{F}_{\mu\nu}=\partial_\mu\tilde{A}_\nu-\partial_\nu\tilde{A}_\mu$. In Eq. (A.12), k is integrated out. As a consequence, C component in the $\exp\left(-k^2/C^2\right)$ term cancels with the C component in the $i/16\pi^2C^2$ term. So, the result is C independent. The action for the chiral anomaly is

$$S_a=\frac{i}{2\pi\nu}\int d\tau dx\Big[e\phi E_x+\frac{1}{4\pi}(\partial_\tau\phi)^2+\frac{\nu}{4\pi}(\partial_x\phi)^2\Big]. \qquad \text{(A.13)}$$

Or, in real-time:

$$S_a=\frac{-1}{2\pi\nu}\int dtdx\Big[e\phi E_x-\frac{1}{4\pi\nu}(\partial_t\phi)^2+\frac{\nu}{4\pi}(\partial_x\phi)^2\Big]. \qquad \text{(A.14)}$$

Appendix B

Detailed calculation of $\mathbf{Tr}\left[\frac{1}{2}G_0 V G_0 V\right]$ (first part)

In Chapter 4, we attempt to calculate $\mathrm{Tr}\left[\frac{1}{2}G_0 V G_0 V\right]$ explicitly, in the appendix, we are performing the detailed calculations. For simplicity, we can write the spatial Fourier component of any function $g(x)$ as

$$\tilde{g}(k) = \frac{1}{\sqrt{\beta N a}} \int dx d\tau e^{i\omega_n \tau + i k_1 x} g(x,\tau), \tag{B.1}$$

and we define $q = (q_0, q_1)$. Since

$$\begin{aligned}\mathrm{Tr}[G_0 V G_0 V] = \frac{1}{\beta N a} \sum_{q_1,q_0} \frac{1}{Na} \sum_{k_1,n,n'} |\langle k_1 n|V(q)|k_1 + q_1 n'\rangle \langle k_1 + q_1 n'|V(-q)|k_1 n\rangle \times \\ \frac{\tilde{f}_{k_1,n} - \tilde{f}_{k_1+q_1,n'}}{\epsilon_{k_1,n} - \epsilon_{k_1+q_1,n'} + i q_0}.\end{aligned} \tag{B.2}$$

We assume the perturbations are small, so the second and higher orders of the perturbations are less important such that B_x^2, B_y^2 and $\tilde{\gamma}^2$ are ignored. How the first order of these perturbations couple with momentum have been studied in the first order expansion except $q_0 \tilde{B_z}$, thus we can also ignore the first order contributions of the perturbations

except for $q_0\tilde{B_z}$ in the second order expansion, so

$$\begin{aligned}\mathrm{Tr}[G_0VG_0V] = \frac{1}{\beta Na}\sum_{q_1\cdot q_0}\frac{1}{Na}\sum_{k_1}\frac{\epsilon_{k_1}+\epsilon_{k_1+q_1}-iq_0}{(\epsilon_{k_1}+\epsilon_{k_1+q_1})^2+q_0^2}\Big(\frac{1}{4}q_0^2\tilde{\phi}(q)\tilde{\phi}^\star(q)\sin^2\left(\frac{\theta_{k_1}+\theta_{k_1'}}{2}\right)\\ +\left(-\frac{1}{4}q_1^2v^2\tilde{\phi}(q)\tilde{\phi}^\star(q)+e^2v^2\tilde{A}_0(q)\tilde{A}_0^\star(q)\right)\sin^2\left(\frac{\theta_{k_1}-\theta_{k_1'}}{2}\right)\\ +e^{v2}\tilde{A}_1(q)\tilde{A}_1^\star(q)\cos^2\left(\frac{\theta_{k_1}+\theta_{k_1'}}{2}\right)\\ +\Big(-\frac{1}{2}q_0\tilde{\phi}(q)ev\tilde{A}_1^\star(q)+\frac{1}{2}q_0\tilde{\phi}^\star(q)\tilde{A}_1(q)\Big)\sin^2\left(\frac{\theta_{k_1}+\theta_{k_1'}}{2}\right)\Big)\\ +\frac{\epsilon_{k_1}+\epsilon_{k_1+q_1}+iq_0}{(\epsilon_{k_1}+\epsilon_{k_1+q_1})^2+q_0^2}\Big(\frac{1}{4}q_0^2\tilde{\phi}(q)\tilde{\phi}(q)^\star\sin^2\left(\frac{\theta_{k_1}+\theta_{k_1'}}{2}\right)\\ +\left(\frac{1}{4}q_1^2v^2\tilde{\phi}(q)\tilde{\phi}(q)^\star-e^2v^2\tilde{A}_0(q)\tilde{A}_0^\star(q)\right)\sin^2\left(\frac{\theta_{k_1}-\theta_{k_1'}}{2}\right)\\ +e^{v2}\tilde{A}_1(q)\tilde{A}_1^\star(q)\cos^2\left(\frac{\theta_{k_1}+\theta_{k_1'}}{2}\right)\\ +\Big(-\frac{1}{2}q_0\tilde{\phi}(q)ev\tilde{A}_1^\star(q)+\frac{1}{2}q_0\tilde{\phi}^\star(q)\tilde{A}_1(q)\Big)\sin^2\left(\frac{\theta_{k_1}+\theta_{k_1'}}{2}\right)\Big),\end{aligned}\tag{B.3}$$

where we only consider linear response and potential V is treated as perturbation , so that field B_x, B_y are very small comparing with the frequency, so we consider $B_x w_n, B_x k_1 = 0$ and $B_y w_n, B_y k_1 = 0$. We also consider $B_z k_1 = 0$ but we keep $B_z\omega_n$ since it is related to the electrical field (recall that B_z is equivalent to $-evA_1$). Recall that $\epsilon_{k_1+q_1} = \sqrt{\Delta_0^2+v^2(k_1+q_1)^2}$ and $\cos\theta_{k_1+q_1} = v(k_1+q_1)/\sqrt{\Delta^2+v^2(k_1+q_1)^2}$ and assuming q_0, q_1 are small comparing to the energy gap. Since for any continuous function

$$F(q_0,q_1) = F(0,0)+\frac{\partial F}{\partial q_0}|_0 q_0+\frac{\partial F}{\partial q_1}|_0 q_1+\frac{1}{2}\frac{\partial^2 F}{\partial q_0^2}|_0 q_0^2+\frac{1}{2}\frac{\partial^2 F}{\partial q_1^2}|_0 q_1^2+\frac{\partial^2 F}{\partial q_0 q_1}|_0 q_0 q_1,\tag{B.4}$$

so

$$\begin{aligned}\mathrm{Tr}[G_0VG_0V] = \frac{1}{\beta Na}\sum_{q_0,q_1}\frac{1}{Na}\sum_{k_1}\frac{\sin^2\theta_{k_1}}{\epsilon_{k_1}}\Big(\frac{1}{4}\tilde{\phi}^\star(0)\tilde{\phi}(0)q_0^2-\frac{1}{2}q_0\tilde{\phi}(q)ev\tilde{A}_1^\star(q)\\ +\frac{1}{2}q_0\tilde{\phi}^\star(q)\tilde{A}_1(q)\Big)+\frac{\cos^2\theta_{k_1}}{\epsilon_{k_1}}e^2v^2\tilde{A}_1(q)\tilde{A}_1^\star(q),\end{aligned}\tag{B.5}$$

since

$$\frac{1}{Na}\sum_{k_1}\frac{1}{4\epsilon_{k_1}}(1-\cos^2(\theta_{k_1}))=\frac{1}{4\pi}\int_0^{\pi/2a}dk_1\frac{\Delta_0^2}{\Delta_0^2+v^2k_1^2}\frac{1}{\sqrt{\Delta_0^2+v^2k_1^2}}\approx\frac{1}{4\pi v} \tag{B.6}$$

$$\begin{aligned}\frac{1}{Na}\sum_{k_1}\frac{1}{4\epsilon_{k_1}}\cos^2(\theta_{k_1})&=-\frac{1}{4\pi v}+\frac{1}{4\pi}\int_0^{\pi/2a}dk_1\ \frac{1}{\sqrt{\Delta_0^2+v^2k_1^2}}\\&\approx-\frac{1}{4\pi v}+\frac{1}{v}\text{arctanh}\left(\frac{2\text{v}^2}{2\text{v}^2+\Delta_0^2}\right),\end{aligned} \tag{B.7}$$

which value represents the smallest inverse of energy which is valid for our calculation, thus

$$\begin{aligned}\text{Tr}[\frac{1}{2}G_0VG_0V]=&\int dxd\tau\frac{1}{8\pi v}(\partial_\tau\phi)^2+\frac{i}{2\pi}e\phi(x)\partial_0A_1\\&-\left[\frac{1}{8\pi v}-\frac{1}{2v}\text{arctanh}\left(\frac{2\text{v}^2}{2\text{v}^2+\Delta_0^2}\right)\right]e^2v^2A_1^2.\end{aligned} \tag{B.8}$$

Appendix C

Detailed calculation of $\mathbf{Tr}\left[\frac{1}{2}G_0 V G_0 V\right]$ (second part)

In Chapter 4, we attempt to calculate $\mathrm{Tr}\left[\frac{1}{2}G_0 V G_0 V\right]$ explicitly, in the appendix, we are performing more detailed calculations. If we calculate the momentum sum first from $-\infty$ to ∞, then we calculate the Matsubara sum, the result is

$$
\begin{aligned}
\mathrm{Tr}\left[\frac{1}{2}G_0 V G_0 V\right] &\simeq \int dx d\tau\ \frac{1}{8\pi v}(\partial_\tau \phi)^2 + \frac{i}{2\pi} e\phi(x)\partial_0 A_1 \\
&-\left[\frac{1}{8\pi v} - \frac{1}{2v}\mathrm{arctanh}\left(\frac{2\mathrm{v}^2}{2\mathrm{v}^2+\Delta_0^2}\right)\right] e^2 v^2 A_1^2 \\
&+ \mathrm{tr}\sum_{q,k} \frac{(ik_0 + vk_1 + \Delta_0\sigma^x)}{k_0^2 + v^2 k_1^2 + \Delta_0^2} \frac{(ik_0 + vk_1 + \Delta_0\sigma^x + iq_0 + vq_1\sigma^z)}{(k_0+q_0)^2 + v^2(k_1+q_1)^2 + \Delta_0^2} \\
&\Big(-\frac{1}{2}v^2 e q_1 \tilde{A}_0(q)\tilde{\phi}^\star(q) + \frac{1}{2}e v^2 q_1 \tilde{A}_0^\star(q)\tilde{\phi}(q) + \frac{1}{4}v^2 q_1^2 \tilde{\phi}(q)\tilde{\phi}^\star(q) + e^2 v^2 \tilde{A}_0(q)\tilde{A}_0^\star(q)\Big) \\
&+ \sum_k \frac{1}{\pi}\int_0^\infty dk_0 dk_1 \frac{(-k_0^2 + v^2 k_1^2 + \Delta_0^2)}{(k_0^2 + v^2 k_1^2 + \Delta_0^2)\left[(k_0+q_0)^2 + v^2(k_1+q_1)^2 + \Delta_0^2\right]} \\
&\Big(-\frac{1}{2}v^2 e q_1 \tilde{A}_0(q)\tilde{\phi}^\star(q) + \frac{1}{2}e v^2 q_1 \tilde{A}_0^\star(q)\tilde{\phi}(q) + \frac{1}{4}v^2 q_1^2 \tilde{\phi}(q)\tilde{\phi}^\star(q) + e^2 v^2 \tilde{A}_0(q)\tilde{A}_0^\star(q)\Big) \\
&= \int d\tau dx\ \frac{1}{8\pi v}(\partial_\tau \phi)^2 + \frac{1}{8\pi} v(\partial_x \phi)^2 + \frac{i}{2\pi} e\phi(x)\partial_0 A_1 - \frac{i}{2\pi} v e\phi\,\partial_1 A_0 \\
&-\left[\frac{1}{8\pi v} - \frac{1}{2v}\mathrm{arctanh}\left(\frac{2\mathrm{v}^2}{2\mathrm{v}^2+\Delta_0^2}\right)\right] e^2 v^2 A_1^2 + \frac{1}{8\pi} v e^2 A_0^2
\end{aligned}
\tag{C.1}
$$

Bibliography

[1] Ramón Aguado. Majorana quasiparticles in condensed matter. *La Rivista del Nuovo Cimento*, 40(11):523–593, 2017.

[2] Amikam Aharoni et al. *Introduction to the Theory of Ferromagnetism*, volume 109. Clarendon Press, 2000.

[3] Alexander Altland and Ben D Simons. *Condensed matter field theory*. Cambridge university press, 2010.

[4] Neil W Ashcroft and N David Mermin. *Solid state physics*. Cengage Learning, 2022.

[5] B Andrei Bernevig, Taylor L Hughes, and Shou-Cheng Zhang. Quantum spin Hall effect and topological phase transition in HgTe quantum wells. *science*, 314(5806):1757–1761, 2006.

[6] Michael Victor Berry. Quantal phase factors accompanying adiabatic changes. *Proceedings of the Royal Society of London. A. Mathematical and Physical Sciences*, 392(1802):45–57, 1984.

[7] Amir O Caldeira and Anthony J Leggett. Path integral approach to quantum brownian motion. *Physica A: Statistical mechanics and its Applications*, 121(3):587–616, 1983.

[8] R.A. Duine. Spintronic. Lecture notes, Utrecht University, 2009.

[9] Ulrich Eckern and A Geier. Microscopic theory of charge-density wave systems. *Zeitschrift für Physik B Condensed Matter*, 65(1):15–27, 1986.

[10] Marcel Franz and Laurens Molenkamp. *Topological insulators*. Elsevier, 2013.

[11] Liang Fu and Charles L Kane. Topological insulators with inversion symmetry. *Physical Review B*, 76(4):045302, 2007.

[12] Kazuo Fujikawa. Path-integral measure for gauge-invariant fermion theories. *Physical Review Letters*, 42(18):1195, 1979.

[13] Kazuo Fujikawa, Kazuo Fujikawa, Hiroshi Suzuki, et al. *Path integrals and quantum anomalies*. Number 122. Oxford University Press on Demand, 2004.

[14] Thierry Giamarchi. *Quantum physics in one dimension*, volume 121. Clarendon press, 2003.

[15] Jeffrey Goldstone and Frank Wilczek. Fractional quantum numbers on solitons. *Physical Review Letters*, 47(14):986, 1981.

[16] George Grüner. The dynamics of charge-density waves. *Reviews of modern physics*, 60(4):1129, 1988.

[17] Martin Hohenadler. Interplay of site and bond electron-phonon coupling in one dimension. *Physical Review Letters*, 117(20):206404, 2016.

[18] Masakatsu Ishikawa and Hajime Takayama. On the phase dynamics of one-dimensional incommensurate charge-density-wave in an electric field. *Progress of theoretical physics*, 79(2):359–372, 1988.

[19] Brian David Josephson. Supercurrents through barriers. *Advances in Physics*, 14(56):419–451, 1965.

[20] Charles L Kane and Eugene J Mele. Quantum spin Hall effect in graphene. *Physical review letters*, 95(22):226801, 2005.

[21] Charles L Kane and Eugene J Mele. Z_2 topological order and the quantum spin hall effect. *Physical review letters*, 95(14):146802, 2005.

[22] Tom Kennedy and Elliott H Lieb. Proof of the Peierls instability in one dimension. In *Condensed Matter Physics and Exactly Soluble Models*, pages 85–88. Springer, 2004.

[23] Takuya Kitagawa, Takashi Oka, Arne Brataas, Liang Fu, and Eugene Demler. Transport properties of nonequilibrium systems under the application of light: Photoinduced quantum hall insulators without Landau levels. *Physical Review B*, 84(23):235108, 2011.

[24] IV Krive and AS Rozhavsky. Evidence for a chiral anomaly in solid state physics. *Physics Letters A*, 113(6):313–317, 1985.

[25] Konstantin K Likharev. *Dynamics of Josephson junctions and circuits*. Routledge, 2022.

[26] Michael E Peskin. *An introduction to quantum field theory*. CRC press, 2018.

[27] Xiao-Liang Qi and Shou-Cheng Zhang. Topological insulators and superconductors. *Reviews of Modern Physics*, 83(4):1057, 2011.

[28] R Rajaraman and John Stewart Bell. On solitons with half integral charge. *Physics Letters B*, 116(2-3):151–154, 1982.

[29] Ralph Roskies and Fidel Schaposnik. Comment on Fujikawa's analysis applied to the Schwinger model. *Physical Review D*, 23(2):558, 1981.

[30] Mark S Rudner and Netanel H Lindner. Floquet topological insulators: from band structure engineering to novel non-equilibrium quantum phenomena. *arXiv preprint arXiv:1909.02008*, 2019.

[31] Todadri Senthil. Symmetry protected topological phases of quantum matter. *arXiv preprint arXiv:1405.4015*, 2014.

[32] Jairo Sinova, T Jungwirth, X Liu, Y Sasaki, JK Furdyna, WA Atkinson, and AH MacDonald. Magnetization relaxation in (ga, mn) as ferromagnetic semiconductors. *Physical Review B*, 69(8):085209, 2004.

[33] WP Su and JR Schrieffer. Soliton dynamics in polyacetylene. *Proceedings of the National Academy of Sciences*, 77(10):5626–5629, 1980.

[34] Zhao-bin Su and B Sakita. Inhomogeneity expansion for the incommensurate charge-density-wave system. *Physical Review B*, 38(11):7421, 1988.

[35] Denny D Tang and Yuan-Jen Lee. *Magnetic memory: fundamentals and technology*. Cambridge University Press, 2010.

[36] David Vanderbilt. *Berry phases in electronic structure theory: electric polarization, orbital magnetization and topological insulators*. Cambridge University Press, 2018.

[37] Huan-Wen Wang, Bo Fu, and Shun-Qing Shen. Helical symmetry breaking and quantum anomaly in massive Dirac fermions. *Physical Review B*, 104(24):L241111, 2021.

[38] Steven Weinberg. *The quantum theory of fields*, volume 2. Cambridge university press, 1995.

[39] Xiao-Gang Wen. *Quantum field theory of many-body systems: from the origin of sound to an origin of light and electrons*. OUP Oxford, 2004.

[40] Edward Witten. Fermion path integrals and topological phases. *Reviews of Modern Physics*, 88(3):035001, 2016.

[41] Victor M Yakovenko and Hsi-Sheng Goan. Influence of magnetic-field-induced spin-density-wave motion and finite temperature on the quantum Hall effect in quasi-one-dimensional conductors: A quantum field theory. *Physical Review B*, 58(16):10648, 1998.

[42] Xiao-Xiao Zhang, Dirk Manske, and Naoto Nagaosa. Ultrafast excitation and topological soliton formation in incommensurate charge density wave states. *Physical Review B*, 104(12):125132, 2021.